A Section 508–conformant HTML version of this article is available at https://doi.org/10.1289/EHP11072.

Oral Exposure to Polystyrene Microplastics of Mice on a Normal or High-Fat Diet and Intestinal and Metabolic Outcomes

Takuro Okamura,[1] Masahide Hamaguchi,[1] Yuka Hasegawa,[1] Yoshitaka Hashimoto,[1] Saori Majima,[1] Takafumi Senmaru,[1] Emi Ushigome,[1] Naoko Nakanishi,[1] Mai Asano,[1] Masahiro Yamazaki,[1] Ryoichi Sasano,[2] Yuki Nakanishi,[3] Hiroshi Seno,[3] Hirohisa Takano,[4] and Michiaki Fukui[1]

[1]Department of Endocrinology and Metabolism, Kyoto Prefectural University of Medicine, Graduate School of Medical Science, Kyoto, Japan
[2]AiSTI Science Co., Ltd., Wakayama, Japan
[3]Department of Gastroenterology and Hepatology, Kyoto University Graduate School of Medicine, Kyoto, Japan
[4]Environmental Health Sciences, Graduate School of Global Environmental Studies, Kyoto University, Kyoto, Japan

Background: Microplastics (MPs) are small particles of plastic (≤5 mm in diameter). In recent years, oral exposure to MPs in living organisms has been a cause of concern. Leaky gut syndrome (LGS), associated with a high-fat diet (HFD) in mice, can increase the entry of foreign substances into the body through the intestinal mucosa.

Objectives: We aimed to evaluate the pathophysiology of intestinal outcomes associated with consuming a high-fat diet and simultaneous intake of MPs, focusing on endocrine and metabolic systems.

Methods: C57BL6/J mice were fed a normal diet (ND) or HFD with or without polystyrene MP for 4 wk to investigate differences in glucose tolerance, intestinal permeability, gut microbiota, as well as metabolites in serum, feces, and liver.

Results: In comparison with HFD mice, mice fed the HFD with MPs had higher blood glucose, serum lipid concentrations, and nonalcoholic fatty liver disease (NAFLD) activity scores. Permeability and goblet cell count of the small intestine (SI) in HFD-fed mice were higher and lower, respectively, than in ND-fed mice. There was no obvious difference in the number of inflammatory cells in the SI lamina propria between mice fed the ND and mice fed the ND with MP, but there were more inflammatory cells and fewer anti-inflammatory cells in mice fed the HFD with MPs in comparison with mice fed the HFD without MPs. The expression of genes related to inflammation, long-chain fatty acid transporter, and Na^+/glucose cotransporter was significantly higher in mice fed the HFD with MPs than in mice fed the HFD without MPs. Furthermore, the genus *Desulfovibrio* was significantly more abundant in the intestines of mice fed the HFD with MPs in comparison with mice fed the HFD without MPs. *Muc2* gene expression was decreased when palmitic acid and microplastics were added to the murine intestinal epithelial cell line MODE-K cells, and Muc2 gene expression was increased when IL-22 was added.

Discussion: Our findings suggest that in this study, MP induced metabolic disturbances, such as diabetes and NAFLD, only in mice fed a high-fat diet. These findings suggest that LGS might have been triggered by HFD, causing MPs to be deposited in the intestinal mucosa, resulting in inflammation of the intestinal mucosal intrinsic layer and thereby altering nutrient absorption. These results highlight the need for reducing oral exposure to MPs through remedial environmental measures to improve metabolic disturbance under high-fat diet conditions. https://doi.org/10.1289/EHP11072

Introduction

Over the past few decades, the use of plastics has increased dramatically.[1] The production, use, and consumption of plastics, which has been ongoing since the 1950s, has caused major environmental problems globally; in 1960, approximately 500,000 tons of production of synthetic fibers were emitted worldwide.[2] The tonnage has since increased exponentially and was 348 million tons in 2017.[3] Approximately 50% of the plastics produced annually is of the disposable type.[4] Thus, the proliferation of plastics in the environment continues at an alarming rate. Plastic particles have been found to be persistent and ubiquitous pollutants in a variety of environments, including seawater, freshwater, soil, and air.[5–9] Plastic accounts for 60%–80% of marine litter,[10] which indicates that some of the plastic spilled due to inadequate management on land is washed up to the shore.

Microplastics (MPs) are small particles of plastic (≤5 mm in diameter). They can be classified into two categories: primary and secondary. Primary MPs are small plastic beads designed for commercial use, such as in toothpaste, facial cleansers, cosmetics, and industrial abrasives.[11] They are also used as raw materials in the manufacture of various commonly used plastic products. Secondary MPs are the plastics that have been discarded into the environment and are gradually degraded and disintegrated by external factors (especially ultraviolet rays and other environmental factors) into small fragments (≤5 mm).[12–14] Plastics have a stable polymeric structure; however, upon discharge into the ocean, they are degraded and miniaturized mainly by photolysis and thermal oxidative degradation.[15] Human exposure to plastics has been considered to occur only through direct use for eating and drinking purposes.[16,17] However, indirect exposure to additives with large hydrophobic properties, which is attributable to the miniaturization of plastics in the environment, and their uptake into the digestive system of organisms, dissolution into digestive juices containing oil, bioaccumulation, and the food chain are routes for the entry of MPs. Such indirect exposures and their routes of entry are considered to have the most significant impact on humans.[18–20] From a toxicological perspective, the route of exposure (oral, respiratory, or dermal) is important, and oral exposure is the main route of uptake for MPs into the body. Exposure to polystyrene MPs (PS-MPs) reduced the reproductive capacity of oysters[21] and induced the expression of antioxidant enzymes in rotifers.[22] In addition to the global threat to environment from MP pollution, the issue of their potential toxicity to humans has raised serious concerns.[23,24] In mammals, a pioneering study on PS-MPs was conducted on mice by Deng et al.[25] who found that daily exposure to 5 or 20 μm of fluorescent PS-MPs resulted in the accumulation of these particles in the liver, kidney, and intestine. Changes in metabolic profiles revealed that 5 μm of PS-MPs affect energy metabolism, lipid metabolism, and oxidative stress in the liver of mice.[25] PS is one of the major polymer types in

Address correspondence to Michiaki Fukui, Department of Endocrinology and Metabolism, Kyoto Prefectural University of Medicine, Graduate School of Medical Science, 465 Kajii-cho, Kamigyo-ku, Kyoto-city, Kyoto 621-8585, Japan. Telephone: +81-75-251-5505; Fax: +81-75-252-3721. Email: michiaki@koto.kpu-m.ac.jp

Supplemental Material is available online (https://doi.org/10.1289/EHP11072).
Received 8 February 2022; Revised 5 January 2023; Accepted 13 January 2023; Published 22 February 2023.

plastic products, along with the accompanying wastes; PS-specific MPs were commonly found in MP fields.[15,26,27] PS-MPs of 0.5–7 μm in diameter have also been widely applied in bioassays to investigate biological interactions and toxicity in living organisms.[28,29,18] Moreover, exposure of C57BL6/J mice to high concentrations of MPs was reported to increase the number and diversity of gut microbiota in the intestine. Inflammation and increased expression of TLR4, AP-1, and IRF5 was reported in the intestines of mice fed high concentrations of MPs.[30]

Dysbiosis has been known to cause thinning of the mucin layer and loosening of the tight junction in the mucosal epithelium of the small intestine, which allowed toxic substances in the intestinal tract to enter the body.[31,32] In a study using mice, oral intake of MPs worsened dysbiosis.[30] Moreover, mice fed a Western diet that includes a lot of fat, that is, a high-fat diet, developed dysbiosis and leaky gut syndrome (LGS).[33,34] However, most of the papers on MP-induced metabolic disturbances have described experiments conducted under normal diet feeding conditions, and the reports conducted under high-fat diet feeding conditions have not been compared with normal diet feeding conditions.[35] Thus, we hypothesized that the toxicity of MPs might be more marked in LGS induced by a high-fat diet than under a normal diet.

On the other hand, disruption of the mucus barrier has been previously reported to change the innate immunity of the intestinal tract.[36] Among the cells involved in innate immunity, innate lymphoid cells (ILCs) are a type of lymphocyte that compose the T cell innate immune system and include ILC1, 2, and 3. They secrete cytokines that respond rapidly to pathogenic tissue damage and are postured to form subsequent adaptive immunity.[37] Disruption of the mucus barrier alters the number of ILC3s, an important regulator of inflammation and infection in the mucosal barrier.[38] ILC3-derived IL-22 maintained intestinal epithelial barrier function.[39–42] On the other hand, in our previous study, we reported that intestinal ILC1 increased in inflammation of the intestinal tract caused by a high-fat diet.[33,43,44] Taken together, to evaluate the inflammation caused by a high-fat diet and MPs in the intestine, it was necessary to evaluate ILC1 and 3 and associated M1/M2 macrophages in the intestinal mucosa.

We have previously shown that changes in diet alter metabolites, gene expression of nutrient transporters, and inflammatory cells in the upper small intestine, i.e., jejunum, in mice.[33,43,44] Furthermore, because it is well known that nutrient absorption occurs primarily in the small intestine,[45] we thought it more appropriate to evaluate the small intestine rather than the large intestine in this study to clarify the relationship between MPs and metabolic disturbances caused by HFD. Moreover, liver is directly connected to the intestinal tract through the portal blood flow, and portal influx of lipopolysaccharide and endotoxin due to impaired intestinal barrier function in the small intestine has been shown to contribute to the development of nonalcoholic fatty liver disease (NAFLD) and nonalcoholic steatohepatitis (NASH).[46,47] Furthermore, because the metabolic syndrome was identified as a strong predictor of fatty liver disease,[48] it is important to evaluate the liver in the study of endocrine and metabolic pathophysiology through the synergistic effects of MPs and HFD. In this study, we aimed to elucidate the pathophysiology of intestinal deterioration associated with consuming a Western diet and simultaneous intake of MPs, focusing on the endocrine and metabolic systems.

Materials and Methods

Mice

All experimental procedures were approved by the Committee for Animal Research, Kyoto Prefectural University of Medicine, Japan (approval number: M2021-61). We purchased 7-wk-old C57BL/6J (wild type) male mice from Shimizu Laboratory Supplies and kept them in a pathogen-free controlled environment. Littermate mice that were born in Shimizu Laboratory Supplies were used in the experiments. The mice were fed a normal diet (ND; 345 kcal/100 g, fat kcal 4.6%; CLEA) or a high-fat diet [HFD; 459 kcal/100 g, 20% protein, 20% carbohydrate, and 60% fat (lard); D12492, Research Diets Inc.] for 4 wk, starting at 8 wk of age, and equal amounts of feed and water were supplied for pair feeding. One mouse was kept per cage. In our previous studies, the group fed the normal diet with MPs added tended to have the lowest food and water intake among the four groups. Therefore, food and water intakes were measured every 3 d, and the food and water intakes of all mice were normalized based on the lowest intake (group fed a normal diet with MPs added). Moreover, in the MP exposure group, carboxyl group-modified fluorescent PS particles (F-K1 050; 0.45–0.53 μm polystyrene COOH; Green Fluorescent Protein (GFP) fluorescence; Merck) were dissolved in water at 1,000 μg/L, and water was provided *ad libitum*.[49,50] Water with dissolved MPs was sonicated at 20 kHz for 15 min, and the jugs were wrapped in aluminum foil to shield them from light. The water was changed every 3 d. To verify whether MPs were uniformly dispersed in the water, we kept the animals in the cage for 3 d; collected 200 μL of water from the jug on days 0, 1, and 2; counted the number of microplastics using a fluorescence microscope (BZ-X710; Keyence); measured the fluorescence intensity of the microplastic using an Orion L microplate luminometer (490 nm excitation, 520 nm emission) (Berthold Detection Systems); and repeated these procedures thrice. The mice were divided into four groups ($n = 10$ per group) according to diet and whether or not they were given MPs. The body weights of the mice were measured weekly. After an overnight fast, the mice were euthanized at 12 wk of age by exposure to anesthesia (4.0 mg/kg midazolam, 0.3 mg/kg medetomidine, and 5.0 mg/kg butorphanol)[51] (Figure 1A).

Analytical Procedures and Glucose and Insulin Tolerance Tests

Twelve-week-old mice were subjected to intraperitoneal glucose tolerance testing (iPGTT) (2 g/kg of body weight) after a 16-h fast (2 d before sacrifice) and insulin tolerance testing (ITT) (0.5 U/kg body weight) after a 5-h fast (3 d before sacrifice). Blood was sampled via the tail vein. Blood glucose was measured using a glucometer (Gultest mintII; Sanwa Kagaku Kenkyusho). iPGTT and ITT were performed in different mice. Blood glucose was monitored 0, 15, 30, 60, and 120 min after injection. The area under the curve (AUC) of the iPGTT and ITT results was analyzed ($n = 5$).

Measurement of Intestinal Permeability

Fluorescein isothiocyanate (FITC)-labeled dextran solution (25 mg/mL, 20 mL/kg per mouse) (Chondrex, Inc.) was administered via oral gavage at 12 wk of age after a 4-h fast (5 d before sacrifice), and blood was collected by retro-orbital puncture before and 3 h after gavage. The collected blood was immediately subjected to density gradient centrifugation at $1{,}500 \times g$ for 15 min. Plasma was collected and diluted with phosphate-buffered saline (PBS) at a ratio of 1:2. Plasma dextran levels were estimated from luminescence measurements using an Orion L microplate luminometer (490 nm excitation, 520 nm emission) (Berthold Detection Systems) ($n = 10$). It was difficult to separate the FITC signal from FITC-dextran and GFP signal from GFP-MP using absorbance spectrometry. Thus, we measured the GFP signal in serum before administration and FITC-Dextran signal 3 h after administration.

We used the plasma signal after FITC-Dextran administration minus the plasma signal before FITC-Dextran administration as a surrogate index of intestinal permeability.

Blood Biochemistry

Blood samples were taken from fasted mice by cardiac puncture during euthanasia, and the serum samples were collected after centrifugation at 14,000 rpm for 10 min at 4°C. The collected serum was stored at −30 °C until they were mailed to the subcontractor. The levels of alanine aminotransferase (ALT) were measured via the standardization support method described by the Japanese Society for Clinical Chemistry.[52] ALT catalyzes the transfer reaction between the α-keto group of α-ketoglutarate and the amino group of L-alanine to produce pyruvate and glutamate. Conjugated to this reaction, lactate dehydrogenase converts β-nicotinamide adenine dinucleotide reduced form (β-NADH) to β-nicotinamide adenine dinucleotide oxidized form (β-NAD) in the presence of the generated pyruvic acid. The rate of decrease of β-NADH at that time was measured at a wavelength of 330–350 nm to obtain the ALT activity value. Triglyceride (TG),[52] nonesterified fatty acid (NEFA),[53] and low-density lipoprotein (LDL)-cholesterol levels[54] were measured via enzymatic methods [TG; glycerol kinase (GK)-GPO • glycerol blanking method; NEFA; Acyl-CoA synthetase; acyl-CoA oxidase-3; methyl-N-ethyl-N-(beta-Hydroxyethyl)aniline; LDL-cholesterol, cholesterol oxidase]. Free glycerol in the sample is eliminated by the reaction of GK and adenosine-5′-diphosphate (ADP), which is generated simultaneously, and is converted to adenosine-5′-triphosphate (ADP) by pyruvate kinase and phosphoenolpyruvate (PEP) and to adenosine triphosphate (ATP) by pyruvate kinase (PK) and PEP. This elimination reaction removes the effect of free glycerol. TG in the sample is then hydrolyzed to glycerol and fatty acids by lipoprotein lipase, and in the presence of ATP, glycerol-3-phosphate is generated from glycerol by the action of GK, simultaneously producing ADP. In the presence of ADP and glucose, glucose-6-phosphate and adenosine-5′-monophosphate are generated by the action of ADP-dependent hexokinase. G-6-P is further converted to 6-phosphogluconate by the action of glucose-6-phosphate dehydrogenase in the presence of β-NAD. The TG concentration is determined by measuring the increase in the amount of β-NADH produced at the same time at a wavelength of 330–350 nm. In the presence of coenzyme A (CoA) and ATP, NEFA in the sample generates acyl-CoA, AMP, and pyrophosphate by the action of acyl-CoA synthase (ACS). The generated acyl-CoA is oxidized by the action of acyl-CoA oxidase, simultaneously generating 2,3-trans-enoyl-CoA and hydrogen peroxide. The generated hydrogen peroxide quantitatively oxidizes and condenses MEHA and 4-aminoantipyrine by the action of peroxidase to produce a blue-violet dye. The NEFA concentration in the sample is determined by measuring the absorbance of this blue-violet color. LDL and calixarene sulfate form a soluble

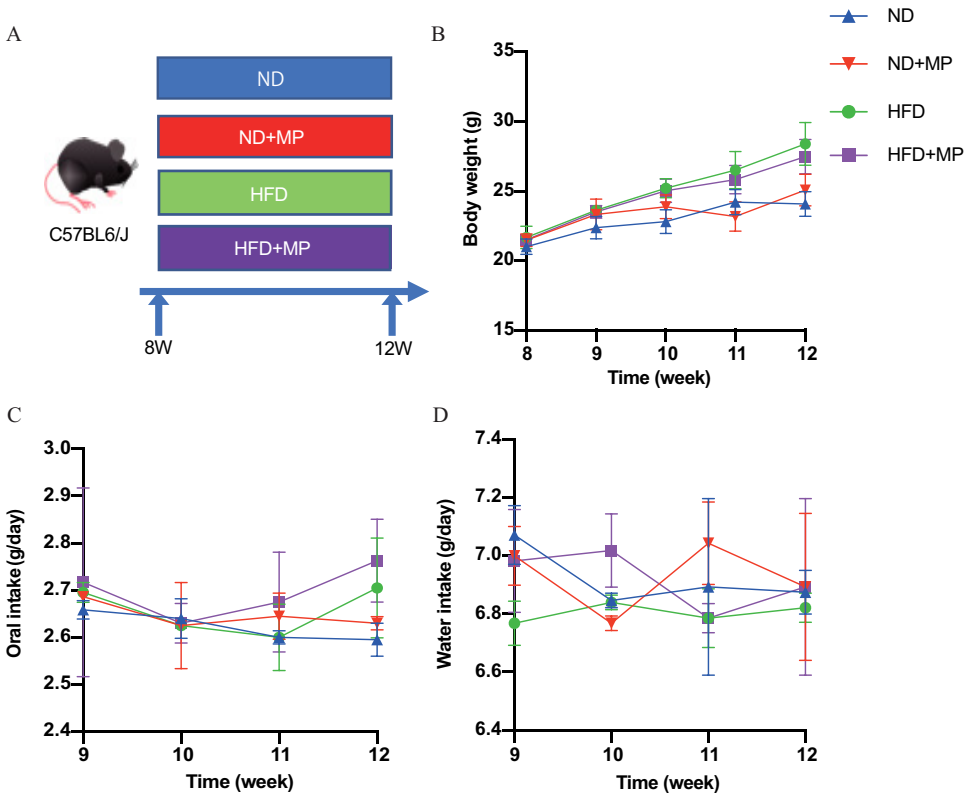

Figure 1. Body weight, food, and water intake; and iPGTT and ITT in mice exposed to ND or HFD ± MPs from 8 wk to 12 wk of age; intestinal permeability in mice exposed to ND or HFD ± MPs at 12 wk of age. (A) Exposure to ND or HFD ± MPs started at 8-weeks of age. (B) Body weight ($n = 10$) and (C and D) intake of food and water over the course of the experiment ($n = 10$). (E and F) Results of iPGTT (2 g/kg body weight) for 12-wk-old mice and the AUC analysis ($n = 5$). Blood glucose was monitored 0, 15, 30, 60, and 120 min after injection. (G and H) Results of ITT (0.75 U/kg body weight) for 12-wk-old mice and the AUC analysis ($n = 5$). Blood glucose was monitored 0, 15, 30, 60, and 120 min after injection. (I) GFP signals from GFP-MP before and after oral gavage of FITC-Dextran for 12-wk-old mice ($n = 10$). Normalized to the levels of ND-fed mice. Data are presented as mean ± SD values. Data were analyzed using one-way ANOVA with Holm-Šídák's multiple comparisons test. $^{*}p < 0.05$, $^{**}p < 0.01$, $^{***}p < 0.001$, and $^{****}p < 0.0001$. Summary data can be found in Table S2. Note: ANOVA, analysis of variance; a.u., arbitrary unit; AUC, area under the curve; FITC, fluorescein isothiocyanate; GFP, green fluorescent protein; HFD, high-fat diet; iPGTT, intraperitoneal glucose tolerance test; ITT, insulin tolerance test; min, minutes; MPs, microplastics; ND, normal diet; SD, standard deviation.

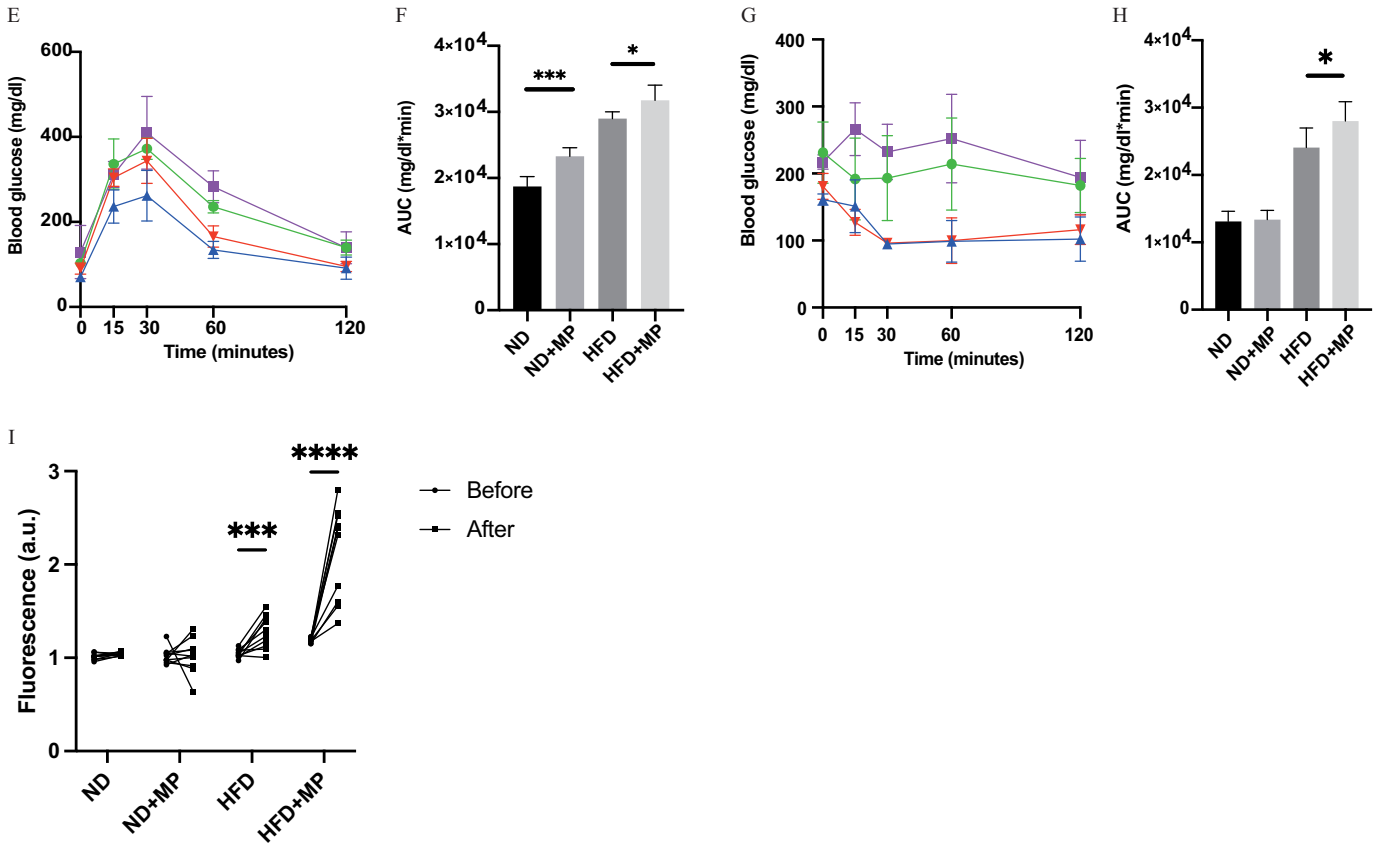

Figure 1. (*Continued.*)

complex and stabilize LDL. The soluble complex is then degraded by intestinal lamina propria (LPL) in the presence of cholic acid. The free ester and free cholesterol are then oxidized in the presence of β-NAD, cholesterol dehydrogenase, and LPL. The amount of β-NADH produced during this process is measured by measuring the absorbance at a wavelength of 330 nm to 350 nm to determine the concentration of LDL-cholesterol in the sample. The biochemical examinations were performed at the FUJIFILM Wako Pure 18 Chemical Corporation ($n = 10$).

Measurement of Free Fatty Acids in Serum, Feces, and Liver Tissues

Collected samples were stored at −30 °C until being used in experiments. Serum (25 μL) obtained via cardiac puncture during euthanasia, feces from the small intestine (15 μg), and liver tissue (15 μg) samples were used for measuring free fatty acids. A fatty acid methylation kit (Nacalai Tesque) was used to analyze the methylation of samples. Gas chromatography–mass spectrometry (GC-MS) was performed using an Agilent 7890B/7000D system (Agilent Technologies) to measure palmitic acid levels in murine sera, feces, and liver tissues ($n = 10$). The final product was loaded onto a Varian capillary column (DB-FATWAX UI; Agilent Technologies). The capillary column used for fatty acid separation was CP-Sil 88 for FAME [100 m × 0.25 mm (inner diameter) × 0.20 μm (membrane thickness); Agilent Technologies]. The column was maintained at 100°C for 4 min, and the temperature was then increased gradually by 3°C/min to 240°C and held for 7 min. The sample was injected in split mode with a split ratio of 5:1. Each fatty acid methyl ester was detected in the selected ion-monitoring mode. All the results were normalized to the peak height for the C17:0 internal standard.[55]

Histology and Immunochemical Analysis of the Small Intestine

Small intestines removed from mice were immediately fixed in 10% buffered formaldehyde for 24 h at 22°C, embedded in paraffin, cut into 4 μm-thick sections, and stained with hematoxylin and eosin (H&E) stain and periodic acid Schiff (PAS) stain with Carnoy's solution. Two pieces of small intestine (one for H&E and one for PAS) were used from each mouse. Images were captured using a fluorescence microscope (BZ-X710; Keyence). The villus height/width and crypt depth were visualized on the H&E–stained sections and were measured at 5 locations per slide for each group of 10 animals using ImageJ software (version 1.53 k; National Institutes of Health). Mucin grains and goblet cells (PAS^+) were enumerated and reported as the average number of goblet cells (PAS^+) per 10 crypts using the ImageJ software, as reported previously ($n = 10$).[56] Moreover, the amount of MP deposition in the intestinal mucosa was evaluated based on the area represented by the green fluorescent protein $(GFP)^+$ region in the slice, and the ratio of the GFP^+ region to the total intestinal epithelial region was calculated (469 nm excitation, 525 nm emission) ($n = 10$). Because the fluorescent dye was stable in the body for 4 d[57] and has been shown to retain up to 50% fluorescence intensity for up to 3 d under ethanol dialysis conditions,[58] small intestine pathology was evaluated 2 d after sacrifice. For immunochemistry, sections of the small intestine were prepared and blocked with Blocking One Histo (Nacalai Tesque, Inc.) for 30 min. Subsequently, the samples were stained with monoclonal primary anti-Muc2 (1/500 dilution; ab272692, Abcam)[59] at 4°C overnight. After washing for 5 min in PBS, the samples were subsequently stained with a Texas-red-conjugated antimouse secondary antibody (1/1,000 dilution; Jackson ImmunoResearch) in the dark at room temperature for 60 min. After washing for 5 min in

PBS, nuclei were stained with 4′,6-diamidino-2-phenylindole (DAPI; Sigma-Aldrich). Images were captured using the BZ-X710 fluorescence microscope (540 nm excitation, 605 nm emission) (Keyence), and the fluorescence intensity of myotube cells was analyzed using ImageJ software ($n = 10$).

Isolation of Mononuclear Cells from the Small Intestine of Mice

To prevent blood contamination in the small intestine, systemic perfusion with heparinized saline was performed before harvesting or washing the tissue with PBS. Samples were stored in cold 2% Fetal Bovine Serum (FBS) with Roswell Park Memorial Institute (RPMI) until being used for experiments. The following experiments were performed on the day of euthanasia. LPL mononuclear cells were isolated using the Lamina Propria Dissociation Kit (130-097-410; Miltenyi Biotec) following the manufacturer's instructions. Cell pellets were resuspended in 5 mL of 40% Percoll® and slowly poured to the upper portion of centrifuge tubes, which contained a bottom layer of 5 mL of 80% Percoll®. Density gradient centrifugation ($420 \times g$, 20 min) was performed, and mononuclear cells in the middle layer were gently extracted with a 1-mL PIPETMAN. The extracted mononuclear cells were washed twice with 2% FBS/PBS.

Tissue Preparation and Flow Cytometry

The cell suspension obtained in the previous section was preincubated with Mouse BD Block purified antimouse CD16/CD32 mAb (394,656; clone: 2.4G2; 1/100; BD Biosciences) for 10 min at 22°C. The following antibodies were used for the gating of the innate lymphoid cells. Cell suspensions were incubated with a mixture of Biotin-CD3e (100,304; clone: 145-2C11; 1/200; eBioscience, Inc.), Biotin-CD45R/B220 (103,204; clone: RA3–6B2; 1/200; eBioscience, Inc.), Biotin-Gr-1 (108,404; clone: RB6-8C5; 1/200; eBioscience), Biotin-CD11c (117,304; clone: N418; 1/200; eBioscience, Inc.), Biotin-CD11b (101,204; clone: M1/70; 1/200; eBioscience, Inc.), Biotin-Ter119 (116,204; clone: TER-119; 1/200; eBioscience, Inc.), Biotin-FceRIa (134,304; clone: MAR-1; 1/200; eBioscience, Inc.), Brilliant Violet 510-Streptavidin (405,233; 1/500; eBioscience, Inc.), PE-Cy7-CD127 (135,014; clone: A7R34; 1/100; eBioscience, Inc.), Pacific Blue-CD45 (103,116; clone: 30-F11; 1/100; eBioscience, Inc.), and Fixable Viability Dye eFluor 780 (1/400; eBioscience, Inc.) for 20 min at 4°C. The cell suspension was washed twice with 2% FBS/PBS and fixed with fixation buffer (420,801; BioLegend, Inc.) for 30 min. After washing with 2% FBS/PBS, the cell suspension was incubated with the mixture of PE-GATA-3 (clone TWAJ, 1/50; eBioscience, Inc.), APC-RORγ (clone AFKJS-9, 1/50, eBioscience, Inc.), and FITC-T-bet (clone 4B10, 1/50; BioLegend, Inc.)[60,61] (Figure S1). We used the following antibodies for gating of M1 and M2 macrophages: FITC-CD206 (MA516870; clone: MR5D3, 1/50, eBioscience, Inc.), PE-F4/80 (12,480,182; clone: BM8, 1/50, eBioscience, Inc.), APC- CD45.2 (17,045,482; clone: 104, 1/50; eBioscience, Inc.), PE-Cy7-CD11c (25,011,482; clone: N418, 1/50, eBioscience, Inc.), and APC-Cy7-CD11b (47,011,282; clone: M1/70, 1/50; eBioscience, Inc.)[62] (Figure S2). We analyzed the stained cells using flow cytometry Canto II, and the data were analyzed using FlowJo (version 10; TreeStar, Inc.) ($n = 10$).

Measurement of Short-Chain Fatty Acids (SCFAs) Levels in the Feces Samples

Samples obtained during euthanasia from the small intestines of mice were stored at −30 °C until being used in experiments. The levels of SCFAs in the feces were analyzed using GC/MS on an Agilent 7890B/7000D system (Agilent Technologies). We homogenized the rectal fecal samples (20 mg) in 500 μL of acetonitrile and 500 μL of distilled water by grinding them (4,000 rpm for 2 min) in a ball mill. We then shook the samples at 1,000 rpm for 30 min at 37°C and centrifuged them at 14,000 rpm for 3 min at room temperature. We separated the supernatant (500 μL), added it to 500 μL of acetonitrile, and shook the mixture at 1,000 rpm for 3 min at 37°C. After centrifugation at 14,000 rpm for 3 min at room temperature, the pH was adjusted to 8 with 0.1 mol/L NaOH, and SCFAs were extracted.

SCFA concentration measurements were automatically measured via GC-MS and an online solid-phase extraction (SPE) method (SGI-M100 SPE-GC system; AiSTI Science Co., Ltd.). After the vials were filled with samples and placed in the autosampler tray, injection into the SPE and GC-MS systems occurred automatically. Solid stratification was performed using Flash-SPE ACXs (AiSTI Science Co., Ltd.). Fifty microliter aliquots of each sample extract were loaded onto the solid phase and rinsed with a 1:1 mixture of water and acetonitrile. Subsequently, the products were dehydrated with acetone, saturated with 4 μL *N-tert*-butyldimethylsilyl-*N*-methyltrifluoroacetamide (MTBSTFA)-toluene solution (1:3), and eluted with hexane after derivatization in the solid phase. Injection of the final product was performed with a programmed temperature vaporizer injector LVI-S250 (AiSTI Science Co., Ltd.). The temperature was maintained at 150°C for 0.5 min, increased gradually to 290°C at a rate of 25°C/min, and then maintained at this temperature for 16 min. A Vf-5ms capillary column [30 m × 0.25 mm (inner diameter) × 0.25 μm (membrane thickness); Agilent Technologies] was used. The column was maintained at 60°C for 3 min, then gradually increased to 100°C at 10°C/min, then to 310°C at 20°C/min, and finally maintained at 310°C for 7 min. The sample was injected in split mode at a ratio of 20:1. Each SCFA was detected in the scan mode (m/z: 70–470). All SCFA results were standardized using the height of the peak of tetradeuteroacetic acid (0.02 nmol/μL)[44] ($n = 10$).

Liver Histology

Liver tissue was obtained, immediately fixed with 10% buffered formaldehyde, and embedded in paraffin. After 24 h of fixation at room temperature, liver sections (4 μm thick) were prepared, and H&E stained. We prepared an Oil Red O stock solution in isopropanol (0.25 g/100 mL) and heated it to 100°C for 10 min. We fixed liver sections with 4% paraformaldehyde for 30 min and then rinsed with PBS. We then prepared a 60% Oil Red O stock solution diluted with distilled water and immersed the sections in the solution for 30 min. We rinsed the stained sections in PBS until the background became clear. We captured the pictures of the liver sections using a BZ-X710 fluorescence microscope (Keyence). Additionally, to assess the severity of NAFLD, we determined the NAFLD activity score (NAS),[63] which is a well-known standard used for measuring the severity of nonalcoholic steatohepatitis (NASH) and changes in NAFLD. The scoring system comprised 14 histological features, of which 4 [steatosis (0–3), lobular inflammation (0–2), hepatocellular ballooning (0–2), and fibrosis (0–4)] were evaluated semiquantitatively ($n = 10$).

Gene Expression Analysis in Murine Jejunum and Liver

The jejunum and liver of mice fasted for 16 h were excised and instantly frozen in liquid nitrogen. The samples were homogenized in ice-cold QIAzol Lysis reagent (Qiagen) at 4,000 rpm for 2 min in a ball mill, and total RNA was extracted according to the manufacturer's instructions and quantified and qualified using the Qubit RNA Assay (Invitrogen). A High-Capacity cDNA

Reverse Transcription Kit (Applied Biosystems) was used for reverse transcription of the total RNA (0.5 μg) to first-strand cDNA, according to the manufacturer's instructions. The mRNA expression levels of *Tnfa*, *Il6*, *Il1b*, *Il22*, *Ffar2*, *Ffar3*, *Cd36*, *Sglt2*, and *Muc2* in the jejunum and of *Tnfa*, *Il6*, *Il1b*, *Scd1*, *Elovl6*, and *Fasn* in the liver were quantified via real-time reverse transcription-polymerase chain reaction (RT-PCR), and TaqMan Fast Advanced Master Mix (Applied Biosystems) was used according to the manufacturer's instructions. The PCR conditions were as follows: 1 cycle of 2 min at 50°C and 20 s at 95°C, followed by 40 cycles of 1 s at 95°C and 20 s at 60°C. The relative expression levels of each target gene were normalized to the *Gapdh* threshold cycle (Ct) values and quantified via the comparative threshold cycle $2^{-\Delta\Delta Ct}$ method. Signals from ND-fed mice were assigned a relative value of 1.0. Expression levels from six mice from each group were determined, and RT-PCR was performed in triplicate for each sample ($n = 10$). Primer sequences (TaqMan probe primers; Applied Biosystems) for each of the genes are presented in Table S1.

16s rRNA Sequencing

A QIAamp DNA Feces Mini Kit (Qiagen) was used for extracting microbial DNA from frozen appendicular fecal samples to ensure sufficient feces volume according to the manufacturer's instructions. The V3-V4 region of the 16S rRNA gene was amplified from DNA using a bacterial universal primer set (341F and 806R). PCR was performed using EF-Taq (Solgent) with 20 ng of genomic DNA as a template in a 30 μL reaction mixture with the following cycles: 95°C for 2 min for activating Taq polymerase, followed by 35 cycles at 95°C, 55°C, and 72°C for 1 min each, and a final 10-min step at 72°C. The amplification products were purified using a multiscreen filter plate (Millipore Corp.). According to the manufacturer's instructions (Macrogen), a MiSeq sequencer (Illumina) was used for 16S rRNA sequencing. For sequence quality filtering, we used QIIME (version 1.9.1).[64] Barcodes or primers with scores of <75% were excluded from the files. Using the UCLUST algorithm at 97% similarity, the number of operational taxonomic units (OTUs) was determined.[65] In addition, BLAST (UNITE 2017) was used for taxonomic assignment of 16S rRNAs with the UNITE sequence set of the Greengenes core set aligned with UCLUST and ITS.

The relative abundances of phyla in the groups were evaluated by one-way analysis of variance (ANOVA) with Holm–Šídák's multiple comparisons test. In addition, alpha diversity (defined as the diversity within an individual sample) was analyzed using the Chao1,[66] Shannon,[67] and Gini–Simpson indices.[68]

The relative abundances of bacterial genera between the groups were evaluated by linear discriminant analysis (LDA) coupled with effect size measurements (LEfSe) (http://huttenhower.sph.harvard.edu/lefse/).[69] With a normalized relative abundance matrix, LEfSe showed taxa with significantly different abundances, and the effect size of the feature was estimated via LDA. A *p*-value threshold of 0.05 (Wilcoxon rank sum test) and an effect size threshold of 2 were used for all biomarkers discussed in this study.

MODE-K Cell Experiments

The murine intestinal epithelial MODE-K cell line (sex: female) was kindly provided by Prof. Richard Blumberg (Harvard Medical School, Boston, USA). MODE-K cells were cultured in Dulbecco's modified Eagle's medium (Nacalai Tesque) supplemented with 10% FBS, 2 mM of glutamine, 100 U/ml penicillin, and 100 μg/mL streptomycin, in an atmosphere of 95% air and 5% CO_2.[70] Cells were spread in 96-well plates at 1×10^4 cells/well, and 1,000 μg/L of MP, 200 μM of palmitic acid (PA),[33] and 50 ng/mL of recombinant mouse IL-22 protein (NBP2-35122, Funakoshi) were added for 24 h on day 5.[71] After 24 h, the cells were then washed twice with cold PBS, detached with 2.5 g/l-Trypsin/1 mmol/l-EDTA solution (Nacalai Tesque), and centrifuged at $300 \times g$ for 5 min at 4°C, and the supernatant was discarded. RT-PCR was performed as described in the "Gene Expression Analysis in Murine Jejunum and Liver" section, and the mRNA expression level of *Muc2* was quantified ($n = 6$). To evaluate the intracellular accumulation of MPs, the pellet was counted after centrifugation. Briefly, 1×10^4 MPs were fractionated and then diluted into 200 μL of PBS. The cell lysate was transferred to a black 96-well plate, and luminescence was measured using an Orion L microplate luminometer (Berthold Detection Systems) ($n = 6$). Signals from cells without MPs, PAs, and IL-22 were assigned a relative value of 1.0.

Statistical Analysis

The data were analyzed using JMP software (version 13.0; SAS Institute, Inc.). One-way ANOVA with Holm–Šídák's multiple comparisons test was used to compare the results of different groups. Statistical significance was set at $p < 0.05$. Figures were generated using GraphPad Prism (version 9.0; GraphPad Software Inc.).

Results

Verification of MP Uniformity in Water

First, to verify whether MPs were uniformly dispersed in the water, we kept the animals in the cage for 3 d with a jug of water, collected 200 μL of water from the jug on days 0, 1, and 2, counted the number of MPs using a fluorescence microscope, and repeated the procedure three times. There were no statistically significant differences in the number and fluorescence intensity of MPs at the three time points, and we considered that MPs were sufficiently available for consumption without fluorescence intensity diminishing or precipitation even under *ad libitum* conditions (Figure S3).

Body Weight, Food and Water Intake, and iPGTT and ITT in Mice Exposed to ND or HFD with and without MPs from 8 Wk to 12 Wk of Age

Body weight and intake of food and water were measured. We observed no difference in the body weight of mice fed a ND and a ND with MPs added and of mice fed a HFD and a HFD with MPs added (Figure 1B). Intake of food and water was not different among the four groups (Figure 1C and 1D). Glucose tolerance was assessed by iPGTT and ITT. In iPGTT, blood glucose levels were higher in mice fed a ND with MPs added and mice fed HFD with MPs added than in both ND and HFD mice (Figure 1E and 1F). On the contrary, in ITT, blood glucose levels were not different between ND and mice fed a ND with MPs added, whereas blood glucose levels in mice fed mice fed a HFD with MPs added were higher than those in mice fed a HFD (Figure 1G and 1H).

Intestinal Permeability in Mice Exposed to ND or High-Fat Diet with and without MPs at 12 Wk of Age

Intestinal permeability was assessed using fluorescent-stained dextran. FITC-labeled dextran was administered orally, and blood was collected before the administration of dextran and 3 h later to measure the plasma GFP-MP and dextran levels as a proxy for intestinal permeability. Because of the interference in signal detection of the GFP-MP accumulation in these mice, we assumed the difference in signal intensity before and 3 h after administration of FITC-dextran represented intestinal permeability and absorbance. There was no difference in GFP signal

between those recorded before and after the administration in the group fed a ND and group fed a ND with MPs, whereas GFP signal after the administration was significantly higher in the group fed an HFD and the group fed an HFD containing MPs in comparison with the signal before the administration (Figure 1I). In addition, the GFP signal was higher in the HFD-fed mice than in the ND-fed mice. There was no significant difference in plasma GFP expression between the ND-fed group and the group fed the ND containing MPs. In contrast, plasma GFP expression was significantly higher in the mice fed an HFD that included MPs than in HFD-fed mice fed an HFD that did not contain MPs (Figure S3D and S3E).

The Serum Levels of Liver Enzymes and Lipids in Mice Exposed to a ND or an HFD with and without MPs at 12 Wk of Age

Next, the serum levels of hepatic enzymes and lipids were investigated. Serum ALT, TG, NEFA, LDL-cholesterol, and palmitic acid levels had no obvious differences between mice fed the ND and the ND containing MPs, whereas the serum levels in mice fed the HFD containing MPs were significantly higher in HFD-fed mice (Figure S4A–E).

Histological Evaluation of Jejunum and Immune Cells Involved in Innate Immunity in LPL of Small Intestine

Histological evaluation of the jejunum was performed. Representative histological images of the jejunum are shown in Figure 2A. We found no obvious differences in the height and width of villi between mice fed ND and ND containing MPs; on the other hand, these parameters in mice fed HFD containing MPs were significantly lower than those in the HFD mice (Figure 2B,C). In addition, exposure to MPs resulted in no apparent difference in crypt depth in ND-fed mice, but crypt depth was significantly higher in mice fed HFD that included MPs than in HFD mice (Figure 2D). The total number of goblet cells was counted in the PAS-stained images. The number of goblet cells in mice fed the ND containing MPs and the those fed HFD containing

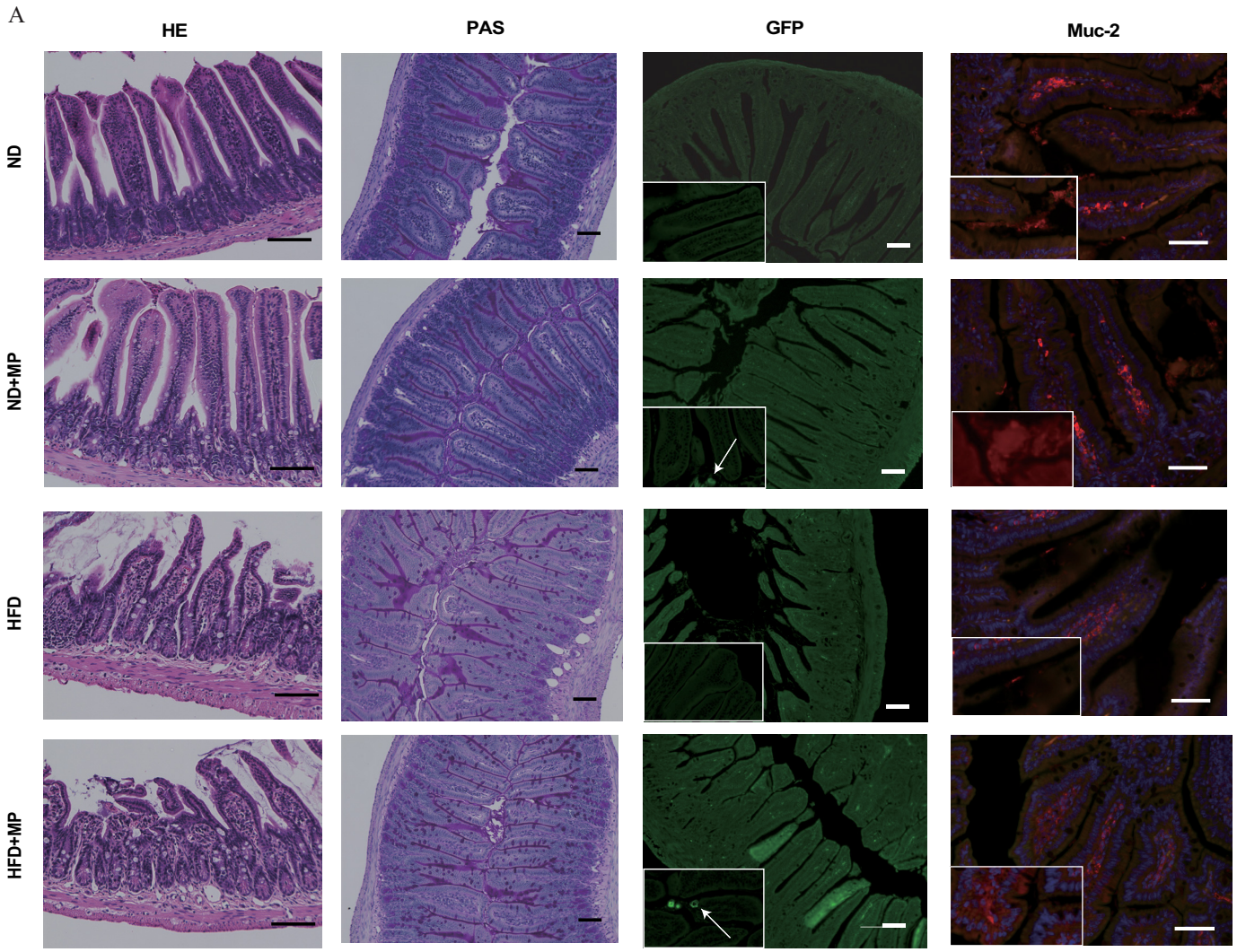

Figure 2. Histological evaluation of jejunum and immune cells involved in innate immunity in LPL of small intestine. (A) Representative images of HE- and PAS-stained, GFP-positive, and Muc2-immunostained jejunum sections. Jejunum tissue was collected at 12 wk of age. In the GFP fluorescence image, MPs are enlarged and indicated by arrows. The scale bars show 100 μm (50 μm for Muc2 image). (B) Villus height ($n = 10$). (C) Villus width ($n = 10$). (D) Crypt depth ($n = 10$). (E) Total goblet cells/area (mm^2 of jejunum) ($n = 10$). (F) Mucus layer thickness ($n = 10$). (G) GFP-positive area ($n = 10$). Ratio of (H) ILC1s to CD45-positive cells, (I) T-bet positive ILC3s to CD45-positive cells, (J) M1 macrophages to M2 macrophages in the small intestine, and (K) ILC3s to CD45-positive cells ($n = 10$ in each case). Data are presented as mean ± SD values. Data were analyzed using one-way ANOVA with Holm-Šídák's multiple comparisons test. Summary data can be found in Table S2. $^{*}p < 0.05$, $^{**}p < 0.01$, $^{***}p < 0.001$, and $^{****}p < 0.0001$. Note: ANOVA, analysis of variance; GFP, green fluorescent protein; H&E, hematoxylin and eosin; HFD, high-fat diet; ILCs, innate lymphoid cells; MPs, microplastics; ND, normal diet; PAS, periodic acid Schiff; SD, standard deviation.

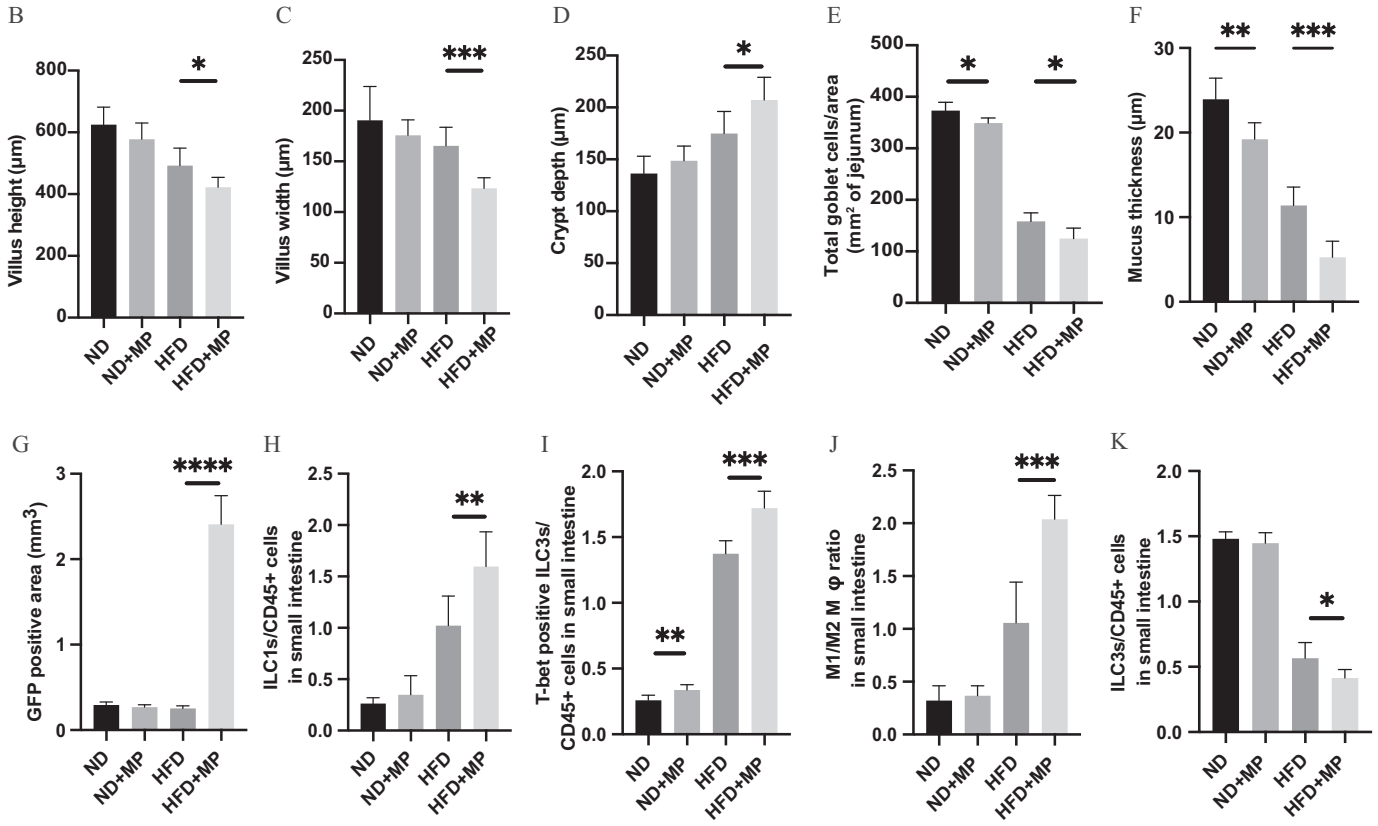

Figure 2. (*Continued.*)

MPs was significantly lower than in ND and HFD mice, respectively (Figure 2E), and mucin layer thickness analyzed by immunochemical staining for Muc2 was smaller in mice fed the ND containing MPs and mice fed the HFD containing MPs in comparison with ND- and HFD-fed mice, respectively (Figure 2F). Moreover, the amount of MP deposition in the intestinal mucosa was calculated based on the area represented by the GFP-positive region in the image. The ratio of GFP-positive region to epithelial region in ND-fed mice did not differ, with or without MP exposure, whereas the ratio of GFP-positive regions was significantly higher in Mice fed HFD containing MPs in comparison with HFD-fed mice (Figure 2G).

Next, the number of cells involved in innate immunity in the LPL of the small intestine was measured by flow cytometry.[33,38,44,72–76] The ratio of ILC1s and T-bet positive ILC3s in CD45+ cells and the ratio of M1 macrophages in M2 macrophages of ND mice were not significantly different from those of mice fed the ND containing MPs; on the other hand, those of mice fed the HFD with MPs were significantly higher than those of HFD-fed mice (Figure 2H,I, and J). Furthermore, there was no significant difference in the ratio of ILC3 cells between mice fed the ND and mice fed the ND containing MPs, but the ratio was lower in the mice fed the HFD containing MPs in comparison with mice fed the HFD that did not contain MPs (Figure 2K).

Metabolites in Feces of Mice Exposed to ND or HFD with and without MPs at 12 Wk of Age

Next, the concentration of the selected metabolites in the feces in the small intestine was determined. Palmitic acid concentrations in feces did not differ between mice fed the ND and mice fed the ND containing MPs, whereas they were lower in the feces of mice fed the HFD containing MPs in comparison with mice fed the HFD that did not contain MPs (Figure 3A). It is notable that the concentration of palmitic acid was considerably higher in mice fed the HFD than in the ND-fed mice, whereas mice fed the HFD containing MPs exhibited levels similar to the ND and mice fed the ND containing MPs. Furthermore, the concentrations of SCFAs such as acetic acid, propanoic acid, and butanoic acid did not differ between ND mice and mice fed the ND containing MPs; on the other hand, they were significantly lower in the feces of mice fed the HFD containing MPs in comparison with HFD-fed mice (Figure 3B–D).

Histological Evaluation of Liver and Palmitic Acid Concentration in Liver of Mice Exposed to the ND or the HFD containing MPs at 12 Wk of Age

The effects of MP on the liver were evaluated. Wet weight of liver was not different between the mice fed the ND and mice fed the ND containing MPs, whereas the weight of mice fed the HFD containing MPs was lower than that of HFD mice (Figure 4A). Although showing a similar trend, the ratio of liver weight to body weight did not differ significantly between ND- and HFD-fed mice, with or without exposure to MPs (Figure 4B). The representative histological images of the liver were shown in Figure 4C. The NAS was zero in ND-fed mice, with and without exposure to MPs, whereas NAS in mice fed the HFD containing MPs was higher than that in mice fed the HFD without MPs (Figure 4D). The area of Oil Red O–stained region was not different between ND-fed mice, with or without exposure to MPs, whereas the area in mice fed the HFD containing MPs was higher than that of HFD-fed mice (Figure 4E). Moreover, palmitic acid concentration in the liver was not different between ND-fed mice, with and without exposure to MPs, but the concentration in mice fed the HFD containing MPs was higher than that in HFD-fed mice (Figure 4F).

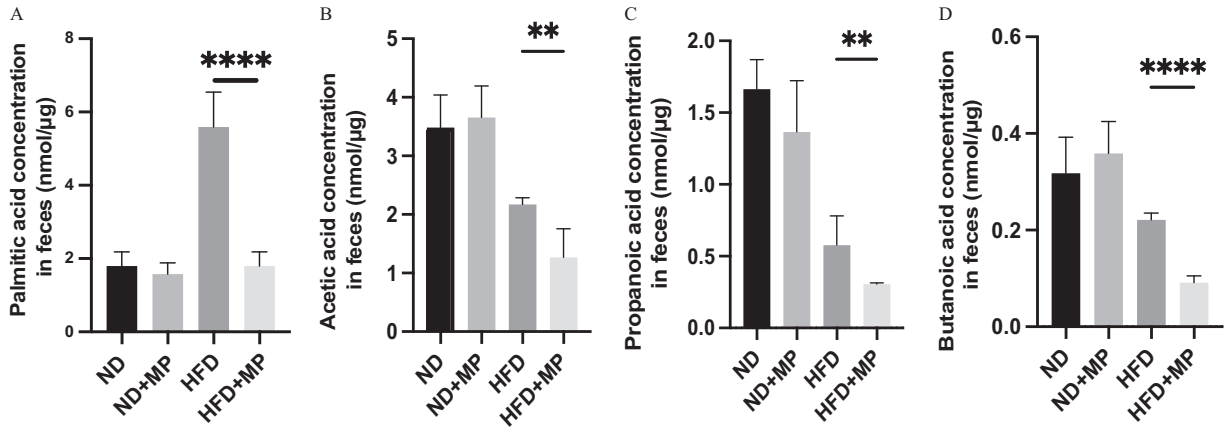

Figure 3. Metabolites in feces of mice exposed to ND or HFD ± MPs at 12 wk of age. The concentrations of (A) palmitic acid, (B) acetic acid, (C) propanoic acid, and (D) butanoic acid in the feces ($n = 10$). Data are presented as mean ± SD values. Data were analyzed using one-way ANOVA with Holm-Šídák's multiple comparisons test. Summary data can be found in Table S2. $^{**}p < 0.01$ and $^{****}p < 0.0001$. Note: ANOVA, analysis of variance; HFD, high-fat diet; MPs, microplastics; ND, normal diet; SD, standard deviation.

Gene Expression in the Small Intestine of Mice Exposed to ND or to the HFD Containing MPs at 12 Wk of Age

Gene expression in small intestine was investigated (Table 1). The relative expression of genes related to inflammation, such as *Tnfa*, *Il6*, and *Il1b*, in small intestine of mice fed the HFD with MPs was higher than that of mice fed the HFD without MPs. The relative expression of *Il22*, a cytokine produced by ILC3, which acts on intestinal epithelial cells and embryonic cells to promote the secretion of antimicrobial peptides and mucus and is involved in the intestinal barrier function,[77] in small intestine of mice fed the HFD with MPs was significantly lower than that of HFD mice. Moreover, the relative expression of *Ffar2* and *Ffar3*, which are free fatty acid receptors that use SCFAs, such as acetic acid, propanoic acid, and butanoic acid as ligands,[78,79] in small intestine of mice fed the HFD with MPs was higher than that of mice fed the HFD without MPs. The relative expression of *Cd36*, which is a long-chain fatty acid transporter, in small intestine of mice fed the HFD with MPs was higher than that of mice fed the HFD without MPs. It is interesting to note that the relative expression of *Sglt1*, a Na^+/glucose cotransporter, in small intestine of mice fed the HFD with MPs was higher than that of mice fed the HFD without MPs. On the other hand, their expressions were not different between ND-fed mice and mice fed the ND with MPs (Table 1).

Gene Expression in the Liver of Mice Exposed to ND or HFD with MPs at 12 Wk of Age

Gene expression in liver was also evaluated. The relative expression of *Tnfa*, *Il6*, and *Il1b* in liver of mice fed the HFD with MPs was higher than that of mice fed the HFD without MPs. Similarly, the relative expression of *Scd1*, *Elovl6*, and *Fasn*, which are fatty acid synthases, in liver of mice fed the HFD with MPs was higher than that in mice fed the HFD without MPs. On the other hand, their expressions were not different between ND mice and mice fed the ND with MPs (Table 1).

16s rRNA Sequence of Gut Microbiota

In 16s rRNA sequence of gut microbiota, the relative abundance of phyla was investigated (Figure 5A). Although there was no clear difference in the relative abundance of phyla between mice fed the ND and mice fed the ND containing MPs, the mice fed the HFD with MPs had a lower abundance of phylum Bacteroidetes and a higher abundance of phylum Proteobactria, in comparison with mice fed the HFD without MPS (Table 2). There was no difference in OTUs between the mice fed the ND and mice fed the ND with MPs and HFD-fed mice and mice fed the HFD with MPs, respectively (Figure 5B). On the other hand, in alpha diversity index, Chao1 index, Shannon index, and Gini-Simpson index in mice fed the HFD with MPs were lower than those in mice fed the HFD without MPs, whereas there was no difference between ND and mice fed the ND with MPs (Figure 5C–E). We also used the LEfSe algorithm to identify the specific taxa that were variably distributed between mice fed the ND without MPs and mice fed the ND with MPs, and between mice fed the HFD without MPS and mice fed the HFD with MPs, respectively. Six taxa were overrepresented (including the phylum Proteobacteria, the genus *Parasutterella*, the family *Sutterellaceae*, the class Betaproteobacteria) and five were underrepresented (including the order Bacteroidales, the class Bacteroidia, the phylum Bacteroidetes, and the genus *Tannerella*) in mice fed the ND with MPs in comparison with that in mice fed the ND without MPs (Figure 5F and H). Moreover, seven taxa were underrepresented (including the family *Prevotellaceae*, the order Bacteroidales, the class Bacteoidia, the phylum Bacteroidetes, the genus *Alloprevotella*, and the family *Ruminococcaceae*) and the genus *Desulfovibrio* were overrepresented in mice fed the HFD with MPs in comparison with that in mice fed the HFD without MPs (Figure 5G and I).

MP and Murine Intestinal Epithelial Cell Line

Using the murine intestinal epithelial cell line MODE-K cells, we investigated the mechanism by which a high-fat diet promotes MP deposition in the small intestinal epithelium. To reproduce the intestinal environment caused by a HFD, PA, a type of saturated fatty acid, was administered to the cells. The mucus that covers and protects the intestinal epithelium is built around its major structural component, the gel-forming MUC2 mucin,[80] and Muc2-deficient mice were shown to have increased intestinal permeability.[81] Therefore, we investigated the expression of *Muc2* by RT-PCR as an indicator of mucin secretion and intestinal permeability. The expression of *Muc2* was not different between control group and MP alone group, whereas the expression in both the PA alone and PA with MPs groups was lower than in the control and MP groups (Figure 6A). In addition, treatment with recombinant protein IL-22, which acts on small intestinal epithelial cells to stimulate secretion of the mucin layer,[77] increased *Muc2* gene expression in both the PA alone and PA with MPs groups, in comparison with that in the nonIL-22-treated group (Figure 6B).

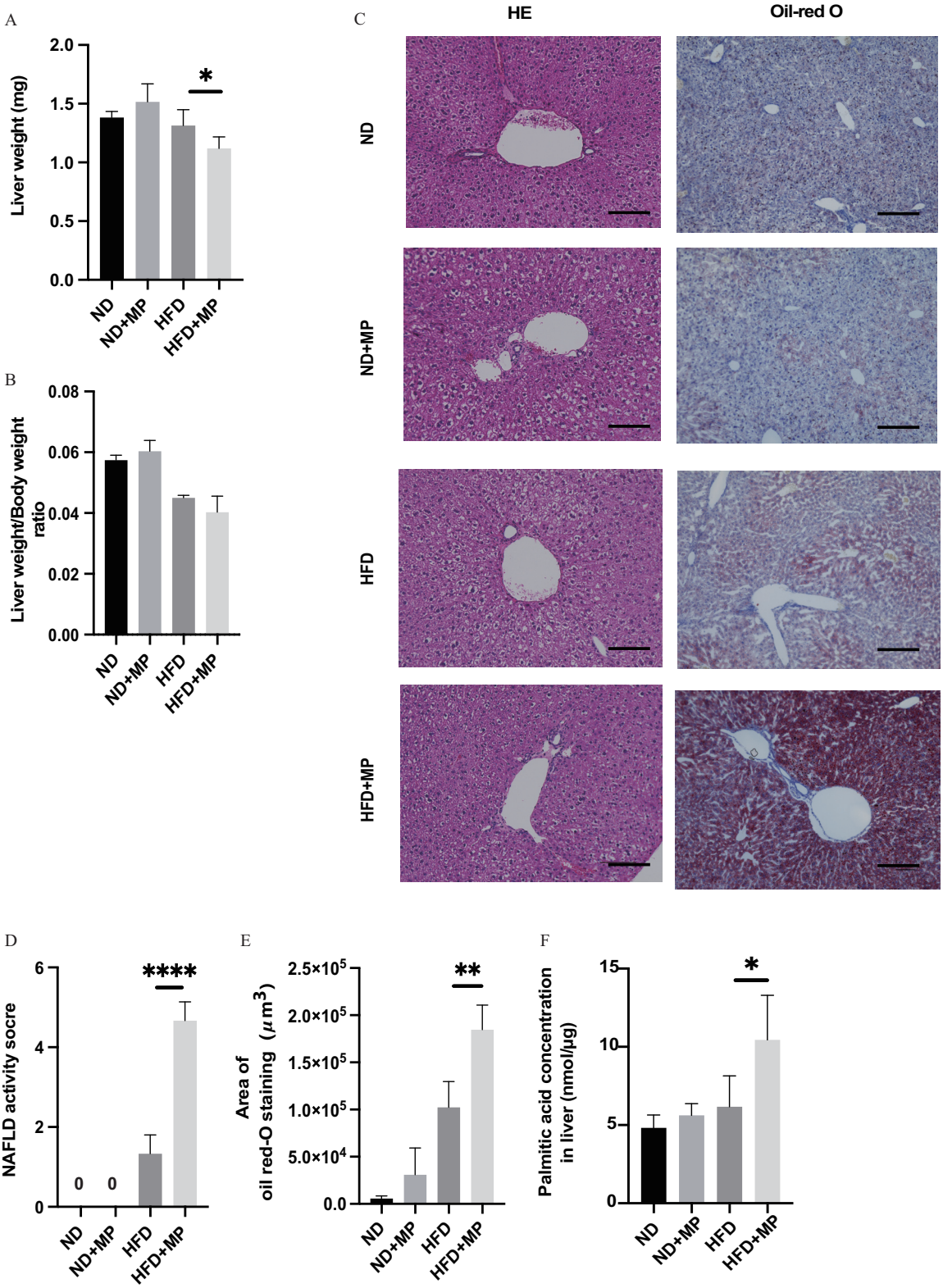

Figure 4. Histological evaluation of liver and palmitic acid concentration in liver of mice exposed to ND or HFD ± MPs at 12 wk of age. (A and B) Absolute and relative liver weight ($n = 10$). (C) Representative images of HE- and Oil Red O–stained liver sections. Liver tissue was collected at 12 wk of age. The scale bars show 100 μm. (D) Nonalcoholic fatty liver disease (NAFLD) activity scores ($n = 10$). (E) Area of Oil Red O–stained region ($n = 10$). (F) The concentration of palmitic acid in the liver ($n = 10$). Data are presented as mean ± SD values. Data were analyzed using one-way ANOVA with Holm-Šídák's multiple comparisons test. Summary data can be found in Table S2. $^{*}p < 0.05$, $^{**}p < 0.01$, and $^{****}p < 0.0001$. Note: HE, hematoxylin & eosin; HFD, high-fat diet; MPs, microplastics; ND, normal diet; SD, standard deviation.

Table 1. Gene expression of small intestine and liver.

Organ	Gene	ND	ND + MP	HFD	HFD + MP
Small intestine	*Tnfa*	1 (0.09)	1.07 (0.04)	1.66 (0.15)*,†	2.53 (0.04)*,†,‡
	Il6	1 (0.18)	0.86 (0.05)	2.58 (0.23)*,†	3.93 (0.06)*,†,‡
	Il1b	1 (0.21)	0.98 (0.13)	2.65 (0.24)*,†	4.04 (0.06)*,†,‡
	Il22	1 (0.18)	0.88 (0.09)	0.47 (0.04)*,†	0.27 (0.08)*,†,‡
	Ffar2	1 (0.02)	0.95 (0.04)	2.43 (0.09)*,†	6.26 (0.13)*,†,‡
	Ffar3	1 (0.05)	0.93 (0.15)	2.45 (0.19)*,†	3.28 (0.11)*,†,‡
	Cd36	1 (0.11)	1.13 (0.06)	1.47 (0.09)*,†	7.63 (2.48)*,†,‡
	Sglt1	1 (0.14)	1.22 (0.28)	2.31 (1.08)*,†	6.11 (0.71)*,†,‡
	Muc2	1 (0.06)	0.97 (0.03)	0.48 (0.14)*,†	0.18 (0.12)*,†,‡
Liver	*Tnfa*	1 (0.21)	1.05 (0.28)	2.44 (0.83)*,†	5.93 (1.18)*,†,‡
	Il6	1 (0.19)	1.01 (0.24)	2.22 (0.36)*,†	5.51 (0.50)*,†,‡
	Il1b	1 (0.19)	1.01 (0.24)	1.66 (0.23)*,†	6.17 (1.72)*,†,‡
	Scd1	1 (0.12)	1.16 (0.09)	1.22 (0.20)*,†	3.03 (0.27)*,†,‡
	Elovl6	1 (0.12)	1.16 (0.09)	1.44 (0.24)*,†	4.28 (0.95)*,†,‡
	Fasn	1 (0.12)	1.16 (0.09)	2.05 (0.09)*,†	9.82 (0.90)*,†,‡

Note: Relative mRNA expression of *Tnfa*, *Il6*, *Il1b*, *Il22*, *Ffar2*, *Ffar3*, *Cd36*, and *Sglt1* in the jejunum normalized to the expression of *Gapdh* ($n = 10$). Relative mRNA expression of *Tnfa*, *Il6*, *Il1b*, *Scd1*, *Elovl6*, and *Fasn* in the liver normalized to the expression of *Gapdh* ($n = 10$). Data are presented as mean ± SD values. The statistical analyses among four groups were performed by one-way ANOVA with Holm-Šídák's multiple comparisons test: *, $p < 0.05$ vs. ND; †, $p < 0.05$ vs. ND+MP; ‡, $p < 0.05$ vs. HFD group. HFD, high-fat diet; MPs, microplastics; ND, normal diet; SD, standard deviation.

Next, the amount of fluorescently labeled MPs accumulated in the cells was measured by absorbance spectrometer. The PA with MPs group accumulated more MP than the MP alone group. However, the accumulation of MP was higher in the MP alone group than in the control group. (Figure 6C). On the other hand, cells treated with IL-22 had significantly less microplastic accumulation in the PA with MPs group in comparison with the MP alone group (Figure 6D).

Discussion

In this study, findings suggestive of metabolic disturbances induced by MP, including deterioration of glucose tolerance and increased fat accumulation in the liver, which were similar to symptoms seen in diabetes and NAFLD, were observed only in mice fed the HFD. Mice fed the HFD with MPs exhibited dysbiosis, thinning of the intestinal mucin layer, indications of inflammation of the intestinal tract, and different gene expression of nutrient transporters in the intestine. To the best of our knowledge, this study is the first to demonstrate that a modern lipid-rich diet and MPs can be associated with findings suggestive of metabolic disturbances, such as diabetes and NAFLD.

MPs are a cause of concern for global pollution and have been found to be toxic to *Mytilus edulis*,[23] fish,[22] and mammals.[24] *In vivo* evidence on the immunotoxicity of MPs suggested that immune cells, including those of the intestinal immune system, might be the targets of plastic-induced damage. Indeed, Li et al.[30] reported that dysbiosis and intestinal inflammation in mice exposed to MPs. Moreover, in a human study, a positive correlation was observed between MPs in feces and the inflammatory bowel disease (IBD) status, indicating that MP exposure might be related to the pathogenesis of IBD or that IBD might exacerbate the retention of MPs.[82] In this study, intestinal permeability was approximated by measuring plasma dextran 4 h after oral administration. We found that plasma dextran was significantly higher in the HFD group in comparison with the ND group and in the mice fed the HFD with MPs in comparison with the mice fed the HFD without MPs, suggesting that intestinal permeability was higher in these groups. In addition, the number of goblet cells was significantly lower in the HFD group in comparison with that in the ND group, and this was even lower in mice exposed to MPs. Pathological images showed very little deposition of MPs in the intestinal mucosa of mice in the ND group unlike in the HFD group. IL-1β and TNF-α were markedly elevated in inflammatory conditions of the intestine, such as IBD.[83,84] Physiological concentrations of IL-1β and TNF-α were associated with markedly increased permeability of tight junctions in intestinal epithelial cells *in vitro*.[85,86] In this study, the expression of IL-1β and TNF-α in small intestine was higher following exposure to MPs. These results suggest that the reduced mucin layer in the HFD-fed mice allowed MPs to enter the intestinal mucosa, causing inflammation in the LPL of the small intestine.

We also analyzed the dynamics of immune cells involved in innate immunity of small intestine. Disruption of the mucosal barrier in mice with colitis altered the number of ILC3s, which are key regulators of inflammation and infection at the mucosal barrier.[87] ILC3-derived IL-22 has been revealed to promote STAT3-dependent expression of antimicrobial peptides and play an important role in maintaining the barrier function of the intestinal epithelium in mice lacking IL-22–producing NKp46+cells.[38–40] Conversely, loss of ILC3s results in decreased expression of IL-22 and reduced levels of antimicrobial peptides expressed by intestinal epithelial cells.[88] ILC3s exhibited plasticity and their function was altered by the expression of the transcription factors RORγt and T-bet in mice with colitis.[41] When stimulated with cytokines, such as IL-12 and IL-18, ex-RORγt-positive ILC3s with T-bet-positive features, that is, ex-ILC3s, increased and RORγt-positive ILC3s decreased, indicating that ILC3s could respond to environmental cues. Previous studies have shown that T-bet-positive ILC3s produced IFN-γ and inhibited the production of IL-17 and IL-22 in mice with inflammatory bowel disease.[75] Thus, T-bet-positive ILC3s exerted a function similar to that of ILC1. ILCs were shown to express receptors for SCFAs, such as G protein–coupled receptor (GPR) 41 [also known as a free fatty acid receptor (FFAR) 3] and GPR43 (FFAR2), which are important for their proliferation, and phosphatidylinositol-3 kinase (PI3K).[89,90] They stimulated the activation of signal transducer and activator of transcription 3 (Stat3), Stat5, and mechanistic target of rapamycin (mTOR) in mice with acute *Clostridium difficile* infection.[91] In fact, several studies of mice,[92,93] rats,[94–96] and humans[97–99] have reported that administration of SCFA improves intestinal inflammation and protected mice from diet-induced obesity and insulin resistance.[93,96,100] Therefore, we hypothesized that the adverse effects of MPs on various metabolic abnormalities may be related to the inflammatory effects of innate immunity by decreasing the production of SCFAs in the gut. Furthermore, in the cell experiments of this study, MODE-K cells, a cell line of small intestinal epithelial cells, when exposed to with IL-22, which is secreted from ILC3 upon stimulation of SCFA, had higher gene expression of Muc2; this expression was lower when cells were exposed to MP and PA treatment, and these cells exhibited significantly lower MP accumulation in the cells. In summary, it is suggested that the production of SCFA enhanced the intestinal barrier function and prevented MP-induced intestinal inflammation, resulting in the induction of various MP-induced metabolic disorders only in the HFD-treated group.

We previously reported that the expression of CD36, a long-chain fatty acid transporter, was reduced in association with the improvement in intestinal inflammation by an increase in SCFAs in mice.[44] In the present study, the expression of CD36 in the small intestine was also significantly higher in mice fed the HFD with MPs in comparison with that in HFD-fed mice. The concentration of palmitic acid, a saturated fatty acid, in fecal excretion was significantly lower in mice fed the HFD with MPs in comparison with that in the other three groups, and the serum and intrahepatic concentrations of palmitic acid were significantly higher, which could be expected to aggravate existing NAFLD. Furthermore, we hypothesized that the MP-induced differences in *Cd36* expression in the small intestine occurred only in the HFD group because the thinning of the mucin layer caused by HFD

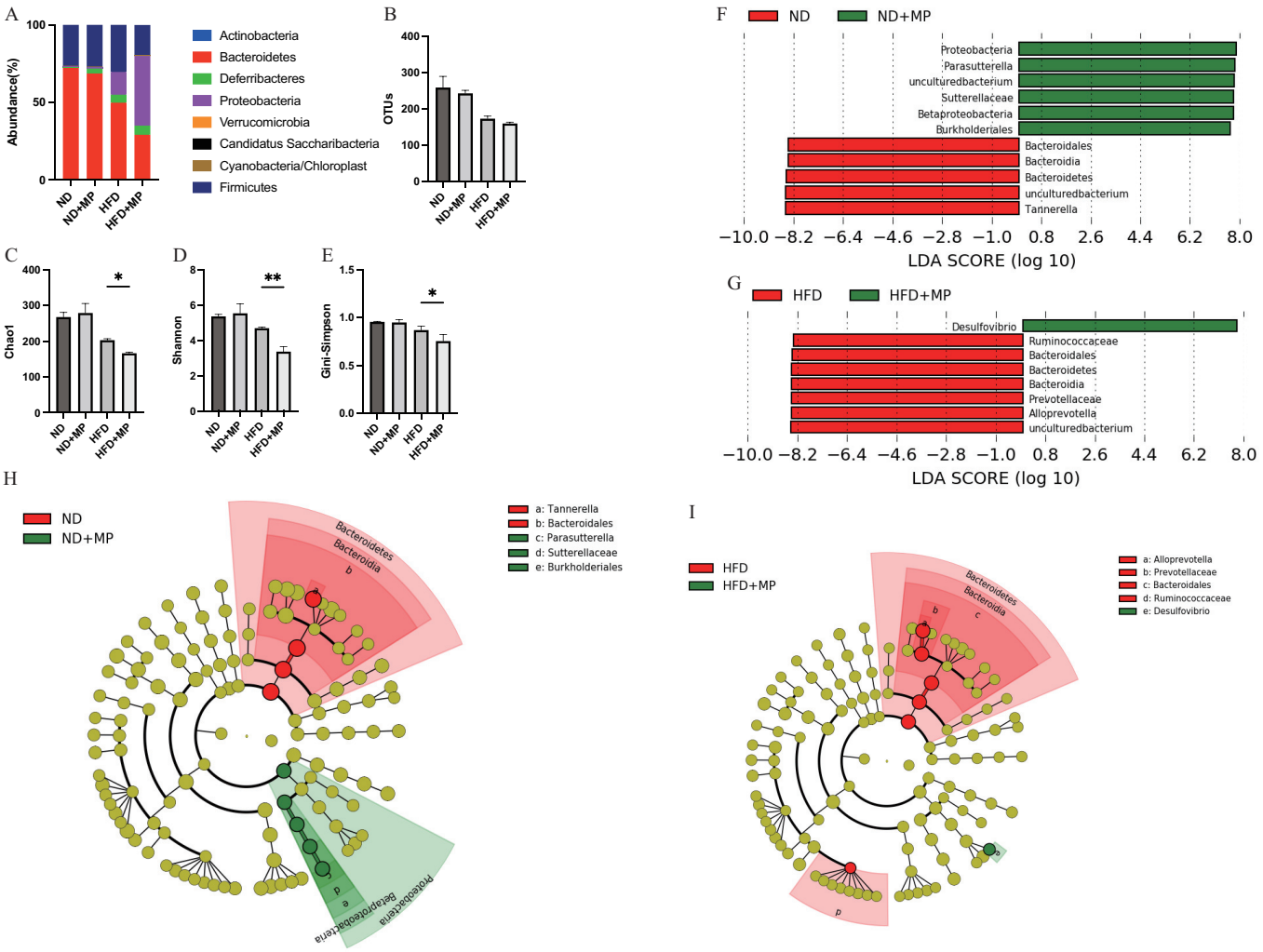

Figure 5. 16s rRNA sequence of gut microbiota of mice exposed to ND or HFD ± MPs at 12 wk of age. (A) The relative abundance of phyla (%). Summary data for this graph shown in Table 2. (B) The number of OTUs ($n = 6$). (C) Chao1 index ($n = 6$). (D) Shannon index ($n = 6$). (E) Gini-Simpson index ($n = 6$). (F and H) LDA score (Log10) and LEfSe cladogram of ND and ND+MP mice; (Red) taxa enriched in ND mice; (Green) taxa enriched in mice fed the ND with MPs ($n = 6$). (G) LDA score and LEfSe cladogram of HFD and mice fed the HFD with MPs; (Red) taxa enriched in HFD mice; (Green) taxa enriched in mice fed the HFD with MPs ($n = 6$). Only taxa with a significant LDA threshold value >2 are shown. Data are presented as mean ± SD values. Data were analyzed using one-way ANOVA with Holm-Šídák's multiple comparisons test. $^{*}p < 0.05$ and $^{**}p < 0.01$. Summary data can be found in Table S2. Note: ANOVA, analysis of variance; HFD, high-fat diet; LDA, linear discriminant analysis; LEfSe, LDA coupled with effect size measurements; MPs, microplastics; ND, normal diet; OTUs, operational taxonomic units; SD, standard deviation.

treatment led to MP deposition in the small intestinal epithelium, which exacerbated the inflammation in the intestinal tract.

In the analyses of gut microbiota, differences in gut microbiota were observed after microplastic administration. The phylum Proteobacteria, the genus *Parasutterella*, the family *Sutterellaceae*, and the class Betaproteobacteria were more frequently present in mice fed the ND with MPs mice than in ND-fed mice. In human study, obese individuals had higher amounts of Proteobacteria and a positive correlation between Proteobacteria and fat intake.[101,102] The family *Sutterellaceae* have been reported to play a part in the

Table 2. The relative abundance of phyla in the feces of mice exposed to ND or HFD ± MPs at 12 wk of age.

	ND		ND + MP			HFD		HFD + MP		
Phylum	Mean (%)	SD	Mean (%)	SD	*p*-Value	Mean (%)	SD	Mean (%)	SD	*p*-Value
Actinobacteria	0.08	0.01	0.05	0.02	0.959	0.05	0.06	0.01	0.02	0.392
Bacteroidetes	71.85	6.18	68.56	10.53	0.859	49.77	2.93	29.12	9.74	0.026
Deferribacteres	0.28	0.05	0.95	0.72	0.847	4.90	2.11	8.65	2.12	0.035
Proteobacteria	0.28	0.07	0.71	0.19	0.995	14.66	6.69	44.98	9.76	0.001
Verrucomicrobia	0.12	0.21	0.22	0.12	0.579	0.01	0.02	0.00	0.00	0.989
Candidatus Saccharibacteria	0.02	0.02	0.01	0.01	0.750	0.00	0.00	0.00	0.00	>0.9999
Cyanobacteria/Chloroplast	0.04	0.03	0.04	0.04	0.990	0.03	0.03	0.01	0.00	0.622
Firmicutes	26.66	5.54	27.17	8.06	0.996	30.30	9.63	19.90	4.65	0.220

Note: Data are presented as mean ± SD values. Data were analyzed using one-way ANOVA with Holm-Šídák's multiple comparisons test. ANOVA, analysis of variance; HFD, high-fat diet; MPs, microplastics; ND, normal diet; SD, standard deviation.

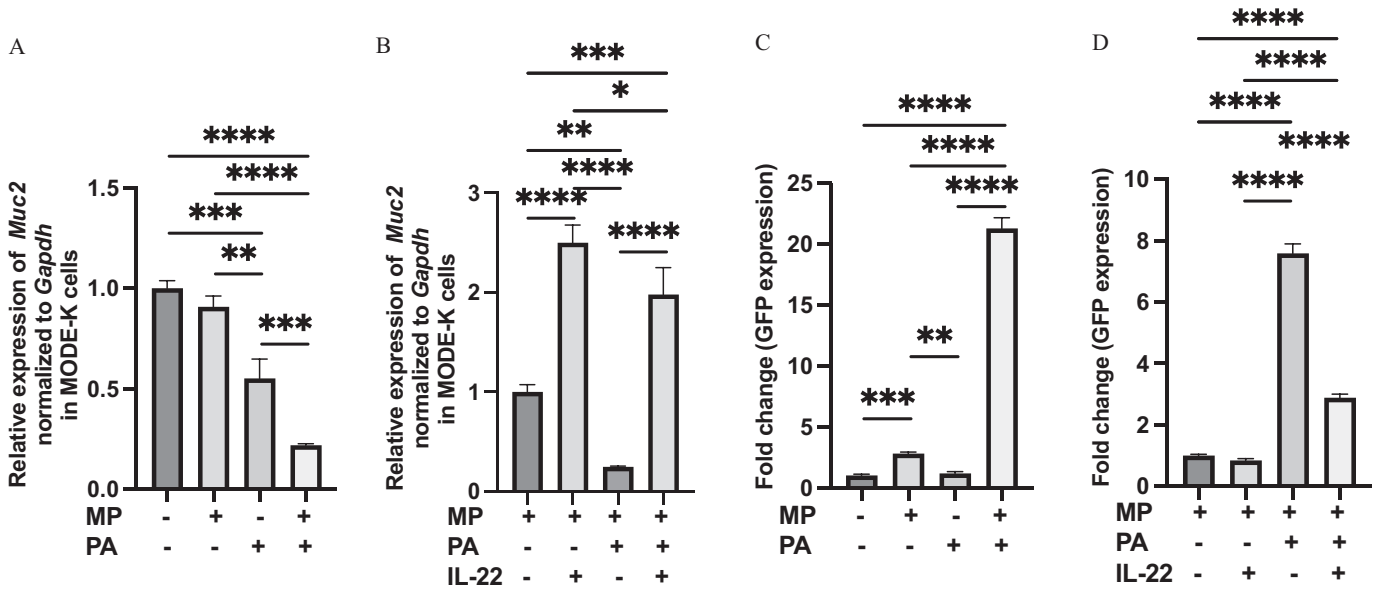

Figure 6. Differences in Muc2 gene expression and MP accumulation in MODE-K cells exposed to MP and saturated fatty acids. (A) Relative mRNA expression of *Muc2* in MODE-K cells without/with MP and PA ($n = 10$). (B) Relative mRNA expression of *Muc2* in MODE-K cells with MP without/with PA and IL-22 ($n = 10$). (C) The fold differences in accumulation of MPs in MODE-K cells without/with MP and PA ($n = 10$). (D) The fold differences in accumulation of MPs in MODE-K cells with MP without/with PA and IL-22 ($n = 10$). Data are presented as mean ± SD values. Data were analyzed using one-way ANOVA with Holm-Šídák's multiple comparisons test. Summary data can be found in Table S2. $^{*}p < 0.05$, $^{**}p < 0.01$, $^{***}p < 0.001$, and $^{****}p < 0.0001$. Note: MP, microplastics; PA, palmitic acid; SD, standard deviation.

pathogenesis of inflammatory bowel disease.[103–105] Moreover, in an animal study, the class Betaproteobacteria was reported to be correlated with weight gain.[106] Taken together, the abundance of gut microbiota involved in dysbiosis was significantly higher in mice fed the ND with MPs than in mice fed the ND without MPs. The phylum Proteobacteria, the genus *Parasutterella*, the family *Sutterellaceae*, and the class Betaproteobacteria were more frequently present in mice fed the HFD with MPs than in ND-fed mice. The family *Prevotellaceae*, the order Bacteroidales, the class Bacteroidia, the phylum Bacteroidetes, the genus *Alloprevotella*, and the family *Ruminococcaceae* were less frequently present in mice fed the HFD with MPs than in mice fed the HFD without MPs. In a human study, the order Bacteroidales, the class Bacteoidia, the phylum Bacteroidetes were associated with weight loss,[107] and the family *Ruminococcaceae* have been described as SCFA producers with beneficial effect on the intestinal barrier in a human study.[108]

Moreover, the genus *Alloprevotella* have been reported to produce acetic acid in a human study[109] and decreased by the administration of HFD in an animal study.[110] On the other hand, it has been observed in several animal models and human studies that the genus *Parasutterella* were significantly reduced by HFD administration.[111–114] The family *Ruminococcaceae* have been reported to be associated with obesity[115] and diabetes[116] in animal studies. Moreover, the genus Desulfovibrio, which was frequently present in the feces of mice fed an HFD with MPs, have been reported to increase in individuals with type II diabetes and obesity[117] and upregulate CD36 expression.[118] In the present study, the expression of *Cd36* in the small intestine of mice fed the HFD with MPs was higher than that of mice fed the HFD without MPs. It was suggested that this alteration of the gut microbiota might have caused various metabolic disorders due to increased absorption of saturated fatty acids from the intestinal tract. Based on these results, the frequency of gut microbiota involved in dysbiosis was higher and that in production of SCFAs was lower in both mice fed the ND with MPs and mice fed the HFD with MPs in comparison with ND- and HFD-fed mice. On the other hand, the diversity of gut microbiota was not different between ND mice and mice fed the ND with MPs, whereas that in mice fed the HFD with MPs was lower than that in HFD-fed mice. Decreased gut microbiota richness have been reported to be associated with various physiological markers of obesity and metabolic syndrome.[119] This decrease might be one possible reason why we did not find differences in metabolic disturbances between ND-fed mice and mice fed the ND with MPs that we observed between HFD-fed mice and mice fed the HFD with MPs, although there were differences in gut microbiota abundance between ND-fed mice and mice fed the ND with MPs.

We also previously showed that HFD-fed wild-type mice experienced dysbiosis glucose intolerance, associated with up-regulation of the expression of Sglt1, a Na^+/glucose cotransporter, in the small intestine.[44] In the present study, the expression of Sglt1 in the small intestine was significantly higher in mice fed the HFD with MPs in comparison with that in HFD-fed mice. An increase in glucose absorption from the small intestine was thought to be one of the reasons for the deterioration in glucose tolerance induced upon exposure to MPs. In contrast, mice fed the ND with MPs did not show significant deterioration in many metabolism-related parameters in comparison with ND-fed mice, but postprandial blood glucose was elevated in the iPGTT and serum lipid levels were higher in the mice fed the ND with MPs than in the group fed only the ND, although the difference was not statistically significant in the present sample size. Considering several reports in zebrafish that oral exposure to MPs increases the deposition of microplastics in the pancreas,[120–122] it is possible that there was a deposition of MPs in the pancreases of mice fed the ND with MPs in this study, which affected the early secretion of insulin. In this study, Red O staining area of the liver was higher in the group fed the ND with MPs than in the ND-only group, although not significantly, suggesting that the ND group was also affected by MP-induced metabolic disturbances to a small extent.

There was a limitation of this study. In iPGTT, we did not measure the plasma insulin levels. If we had had the data, more accurate assessment of insulin resistance would have been possible. In addition, the evaluation of dose response and verification with other size and concentration combinations of microplastics has not been conducted, and this is a future research topic.

In conclusion, to the best of our knowledge, the present study is the first to suggest that MPs cause metabolic disturbances under HFD intake conditions, characteristic of a modern diet. Changes in nutrient absorption might be involved in promoting an inflammatory shift of innate immunity in the intestine, accompanied by the deposition of MPs in the intestinal mucosa and a decrease in SCFA production. This study highlights the need for reducing oral exposure to MPs through remedial environmental measures to improve metabolic disturbances under HFD conditions. Further clinical studies are needed to assess the translational potential of the reported findings for metabolic disturbances.

Acknowledgments

The authors thank all the staff members of the Kyoto Prefectural University of Medicine. The authors also thank Editage (www.editage.com) for English-language editing.

T. O. originated and designed the study, researched the data, and wrote the manuscript. M.H. and Y.H. originated and designed the study, researched the data, and reviewed the manuscript. Y.H., S.M., T.S., E.U., N.N., M.A., and M.Y. researched the data and contributed to the discussion. R.S., Y.N., H.S., and H.T. provided technical cooperation. H.T. and M.F. originated and designed the study, researched the data, and reviewed and edited the manuscript. M.F. is the guarantor of this work and, as such, had full access to all data in the study and takes responsibility for the integrity of the data and the accuracy of the data analysis. All authors were involved in the writing of the manuscript and approved the final version of this article.

This study is supported by JST-CREST (JPMJCR19H3).

The authors declare the following funding received outside the submitted work: M.H. has received grants from Asahi Kasei Pharma, Nippon Boehringer Ingelheim Co., Ltd.; Mitsubishi Tanabe Pharma Corporation; Daiichi Sankyo Co., Ltd.; Sanofi K.K.; Takeda Pharmaceutical Co., Ltd.; Astellas Pharma Inc.; Kyowa Kirin Co., Ltd.; Sumitomo Dainippon Pharma Co., Ltd.; Novo Nordisk Pharma Ltd.; and Eli Lilly Japan K.K.

The authors declare the following funding received outside the submitted work: Y.H. has received grants from Kowa company Ltd.; Takeda Pharmaceutical Co., Ltd.; Ono Pharmaceutical Co., Ltd.; Sumitomo Dainippon Pharma Co., Ltd.; personal fees from Daiichi Sankyo Co., Ltd.; personal fees from Mitsubishi Tanabe Pharma Corp.; personal fees from Sanofi K.K.; and personal fees from Novo Nordisk Pharma Ltd.

The authors declare the following funding received outside the submitted work: T.S. has received personal fees from Ono Pharma Co., Ltd.; Mitsubishi Tanabe Pharma Co.; Astellas Pharma Inc.; Kyowa Hakko Kirin Co., Ltd.; Sanofi K.K.; MSD K.K.; Kowa Pharmaceuticals Co., Ltd.; Taisho Toyama Pharma Co., Ltd.; Takeda Pharma Co., Ltd.; Kissei Pharma Co., Ltd.; Novo Nordisk Pharma Ltd.; and Eli Lilly Japan K.K.

The authors declare the following funding received outside the submitted work: E.U. has received grants from the Japanese Study Group for Physiology and Management of Blood Pressure and the Astellas Foundation for Research on Metabolic Disorders and personal fees from AstraZeneca PLC; Astellas Pharma Inc.; Daiichi Sankyo Co., Ltd.; Kowa Pharmaceuticals Co., Ltd.; MSD K.K.; Mitsubishi Tanabe Pharma Corp.; Novo Nordisk Pharma Ltd.; Taisho Toyama Pharmaceutical Co., Ltd.; Nippon Boehringer Ingelheim Co., Ltd.; and Sumitomo Dainippon Pharma Co., Ltd., outside the submitted work. M.A. received personal fees from Novo Nordisk Pharma Ltd.; Abbott Japan Co., Ltd.; AstraZeneca PLC; Kowa Pharmaceutical Co., Ltd.; Ono Pharmaceutical Co., Ltd.; and Takeda Pharmaceutical Co., Ltd.

The authors declare the following funding received outside the submitted work: M.Y. reports personal fees from MSD K.K.; Sumitomo Dainippon Pharma Co., Ltd.; Kowa Phramaceutical Co., Ltd.; AstraZeneca PLC; Takeda Pharmaceutical Co., Ltd.; Kyowa Hakko Kirin Co., Ltd.; Daiichi Sankyo Co., Ltd.; Kowa Pharmaceuticals Co., Ltd.; and Ono Pharma Co., Ltd.

The authors declare the following funding received outside the submitted work: M.F. has received grants from Nippon Boehringer Ingelheim Co., Ltd.; Kissei Pharma Co., Ltd.; Mitsubishi Tanabe Pharma Co.; Daiichi Sankyo Co., Ltd.; Sanofi K.K.; Takeda Pharma Co., Ltd.; Astellas Pharma Inc.; MSD K.K.; Kyowa Hakko Kirin Co., Ltd., Sumitomo Dainippon Pharma Co., Ltd.; Kowa Pharmaceuticals Co., Ltd.; Novo Nordisk Pharma Ltd., Ono Pharma Co., Ltd.; Sanwa Kagaku Kenkyusho Co., Ltd.; Eli Lilly Japan K.K.; Taisho Pharma Co., Ltd.; Terumo Co.; Teijin Pharma Ltd.; Nippon Chemiphar Co., Ltd.; and Johnson & Johnson K.K. Medical Co.; Abbott Japan Co., Ltd.; and received personal fees from Nippon Boehringer Ingelheim Co., Ltd.; Kissei Pharma Co., Ltd.; Mitsubishi Tanabe Pharma Corp.; Daiichi Sankyo Co.; Ltd., Sanofi K.K.; Takeda Pharma Co., Ltd.; Astellas Pharma Inc.; MSD K.K.; Kyowa Kirin Co., Ltd.; Sumitomo Dainippon Pharma Co., Ltd.; Kowa Pharmaceuticals Co., Ltd.; Novo Nordisk Pharma Ltd.; Ono Pharma Co., Ltd.; Sanwa Kagaku Kenkyusho Co., Ltd.; Eli Lilly Japan K.K.; Taisho Pharma Co., Ltd.; Bayer Yakuhin, Ltd.; AstraZeneca K.K.; Mochida Pharma Co., Ltd.; Abbott Japan Co., Ltd.; Medtronic Japan Co., Ltd.; Arkley Inc.; Teijin Pharma Ltd.; and Nipro Corp.

References

1. Geyer R, Jambeck JR, Law KL. 2017. Production, use, and fate of all plastics ever made. Sci Adv 3(7):e1700782, PMID: 28776036, https://doi.org/10.1126/SCIADV.1700782.
2. Wu P, Huang J, Zheng Y, Yang Y, Zhang Y, He F, et al. 2019. Environmental occurrences, fate, and impacts of microplastics. Ecotoxicol Environ Saf 184:109612, PMID: 31476450, https://doi.org/10.1016/J.ECOENV.2019.109612.
3. Plastics-the Facts 2018 An analysis of European plastics production, demand and waste data.
4. UNEP (United Nations Environmental Programme). Single-Use Plastics: A Roadmap for Sustainability | International Environmental Technology Centre. https://www.unep.org/ietc/ja/node/53?%2Fresources%2Fpublication%2Fsingle-use-plastics-roadmap-sustainability= [accessed 3 May 2022].
5. Alimba CG, Faggio C. 2019. Microplastics in the marine environment: current trends in environmental pollution and mechanisms of toxicological profile. Environ Toxicol Pharmacol 68:61–74, PMID: 30877952, https://doi.org/10.1016/j.etap.2019.03.001.
6. Ferreira I, Venâncio C, Lopes I, Oliveira M. 2019. Nanoplastics and marine organisms: what has been studied? Environ Toxicol Pharmacol 67:1–7, PMID: 30685594, https://doi.org/10.1016/j.etap.2019.01.006.
7. Koelmans AA, Mohamed Nor NH, Hermsen E, Kooi M, Mintenig SM, de France J. 2019. Microplastics in freshwaters and drinking water: critical review and assessment of data quality. Water Res 155:410–422, PMID: 30861380, https://doi.org/10.1016/j.watres.2019.02.054.
8. Rillig MC. 2012. Microplastic in terrestrial ecosystems and the soil? Environ Sci Technol 46(12):6453–6454, PMID: 22676039, https://doi.org/10.1021/es302011r.
9. Prata JC. 2018. Airborne microplastics: consequences to human health? Environ Pollut 234:115–126, PMID: 29172041, https://doi.org/10.1016/j.envpol.2017.11.043.
10. Derraik JGB. 2002. The pollution of the marine environment by plastic debris: a review. Mar Pollut Bull 44(9):842–852, PMID: 12405208, https://doi.org/10.1016/S0025-326X(02)00220-5.
11. Boucher J, Friot D. 2017. Primary Microplastics in the Oceans: A Global Evaluation of Sources. Gland, Switzerland: IUCN. https://doi.org/10.2305/IUCN.CH.2017.01.en.
12. Cooper DA, Corcoran PL. 2010. Effects of mechanical and chemical processes on the degradation of plastic beach debris on the island of Kauai, Hawaii. Mar Pollut Bull 60(5):650–654, PMID: 20106491, https://doi.org/10.1016/j.marpolbul.2009.12.026.
13. Yakimets I, Lai D, Guigon M. 2004. Effect of photo-oxidation cracks on behaviour of thick polypropylene samples. Polym Degrad Stab 1(86):59–67, https://doi.org/10.1016/J.POLYMDEGRADSTAB.2004.01.013.
14. Turton TJ, White JR. 2001. Effect of stabilizer and pigment on photo-degradation depth profiles in polypropylene. Polym Degrad Stab 74(3):559–568, https://doi.org/10.1016/S0141-3910(01)00193-8.

15. Andrady AL. 2011. Microplastics in the marine environment. Mar Pollut Bull 62(8):1596–1605, PMID: 21742351, https://doi.org/10.1016/j.marpolbul.2011.05.030.
16. Mason SA, Welch VG, Neratko J. 2018. Synthetic polymer contamination in bottled water. Front Chem 6:407, PMID: 30255015, https://doi.org/10.3389/FCHEM.2018.00407.
17. Schymanski D, Goldbeck C, Humpf HU, Fürst P. 2018. Analysis of microplastics in water by micro-Raman spectroscopy: release of plastic particles from different packaging into mineral water. Water Res 129:154–162, PMID: 29145085, https://doi.org/10.1016/j.watres.2017.11.011.
18. Farrell P, Nelson K. 2013. Trophic level transfer of microplastic: M*ytilus edulis* (L.) to *Carcinus maenas* (L.). Environ Pollut 177:1–3, PMID: 23434827, https://doi.org/10.1016/j.envpol.2013.01.046.
19. Nelms SE, Galloway TS, Godley BJ, Jarvis DS, Lindeque PK. 2018. Investigating microplastic trophic transfer in marine top predators. Environ Pollut 238:999–1007, PMID: 29477242, https://doi.org/10.1016/j.envpol.2018.02.016.
20. Zhao S, Ward JE, Danley M, Mincer TJ. 2018. Field-based evidence for microplastic in marine aggregates and mussels: implications for trophic transfer. Environ Sci Technol 52(19):11038–11048, PMID: 30156835, https://doi.org/10.1021/acs.est.8b03467.
21. Sussarellu R, Suquet M, Thomas Y, Lambert C, Fabioux C, Pernet MEJ, et al. 2016. Oyster reproduction is affected by exposure to polystyrene microplastics. Proc Natl Acad Sci U S A 113(9):2430–2435, PMID: 26831072, https://doi.org/10.1073/pnas.1519019113.
22. Jeong C-B, Won E-J, Kang H-M, Lee M-C, Hwang D-S, Hwang U-K, et al. 2016. Microplastic size-dependent toxicity, oxidative stress induction, and p-JNK and p-p38 activation in the monogonont rotifer (*Brachionus koreanus*). Environ Sci Technol 50(16):8849–8857, PMID: 27438693, https://doi.org/10.1021/acs.est.6b01441.
23. Rochman CM, Browne MA, Halpern BS, Hentschel BT, Hoh E, Karapanagioti HK, et al. 2013. Policy: classify plastic waste as hazardous. Nature 494(7436):169–171, PMID: 23407523, https://doi.org/10.1038/494169a.
24. Browne MA, Dissanayake A, Galloway TS, Lowe DM, Thompson RC. 2008. Ingested microscopic plastic translocates to the circulatory system of the mussel, *Mytilus edulis* (L). Environ Sci Technol 42(13):5026–5031, PMID: 18678044, https://doi.org/10.1021/es800249a.
25. Deng Y, Zhang Y, Lemos B, Ren H. 2017. Tissue accumulation of microplastics in mice and biomarker responses suggest widespread health risks of exposure. Sci Rep 7:46687, PMID: 28436478, https://doi.org/10.1038/SREP46687.
26. Faure F, Demars C, Wieser O, Kunz M, de Alencastro LF. 2015. Plastic pollution in Swiss surface waters: nature and concentrations, interaction with pollutants. Environ Chem 12(5):582–591, https://doi.org/10.1071/EN14218.
27. Di M, Wang J. 2018. Microplastics in surface waters and sediments of the Three Gorges Reservoir, China. Sci Total Environ 616–617:1620–1627, PMID: 29050832, https://doi.org/10.1016/j.scitotenv.2017.10.150.
28. Cole M, Lindeque P, Fileman E, Halsband C, Goodhead R, Moger J, et al. 2013. Microplastic ingestion by zooplankton. Environ Sci Technol 47(12):6646–6655, PMID: 23692270, https://doi.org/10.1021/es400663f.
29. Lei L, Liu M, Song Y, et al. 2018. Polystyrene (nano)microplastics cause size-dependent neurotoxicity, oxidative damage and other adverse effects in *Caenorhabditis elegans*. Environ Sci Nano 5(8):2009–2020, https://doi.org/10.1039/C8EN00412A.
30. Li B, Ding Y, Cheng X, Sheng D, Xu Z, Rong Q, et al. 2020. Polyethylene microplastics affect the distribution of gut microbiota and inflammation development in mice. Chemosphere 244:125492, PMID: 31809927, https://doi.org/10.1016/J.CHEMOSPHERE.2019.125492.
31. Ghosh SS, Wang J, Yannie PJ, Ghosh S. 2020. Intestinal barrier dysfunction, LPS translocation, and disease development. J Endocr Soc 4(2):bvz039, PMID: 32099951, https://doi.org/10.1210/JENDSO/BVZ039.
32. Vancamelbeke M, Vermeire S. 2017. The intestinal barrier: a fundamental role in health and disease. Expert Rev Gastroenterol Hepatol 11(9):821–834, PMID: 28650209, https://doi.org/10.1080/17474124.2017.1343143.
33. Okamura T, Hashimoto Y, Majima S, Senmaru T, Ushigome E, Nakanishi N, et al. 2021. Trans fatty acid intake induces intestinal inflammation and impaired glucose tolerance. Front Immunol 12:669672, PMID: 33995404, https://doi.org/10.3389/fimmu.2021.669672.
34. Cheng L, Jin H, Qiang Y, Wu S, Yan C, Han M, et al. 2016. High fat diet exacerbates dextran sulfate sodium induced colitis through disturbing mucosal dendritic cell homeostasis. Int Immunopharmacol 40:1–10, PMID: 27567245, https://doi.org/10.1016/j.intimp.2016.08.018.
35. Li L, Xu M, He C, Wang H, Hu Q. 2022. Polystyrene nanoplastics potentiate the development of hepatic fibrosis in high fat diet fed mice. Environ Toxicol 37(2):362–372, PMID: 34755918, https://doi.org/10.1002/tox.23404.
36. Constantinides MG, McDonald BD, Verhoef PA, Bendelac A. 2014. A committed precursor to innate lymphoid cells. Nature 508(7496):397–401, PMID: 24509713, https://doi.org/10.1038/nature13047.
37. Bando JK, Colonna M. 2016. Innate lymphoid cell function in the context of adaptive immunity. Nat Immunol 17(7):783–789, PMID: 27328008, https://doi.org/10.1038/ni.3484.
38. Satoh-Takayama N, Vosshenrich CAJ, Lesjean-Pottier S, Sawa S, Lochner M, Rattis F, et al. 2008. Microbial flora drives interleukin 22 production in intestinal NKp46+ cells that provide innate mucosal immune defense. Immunity 29(6):958–970, PMID: 19084435, https://doi.org/10.1016/j.immuni.2008.11.001.
39. Sonnenberg GF, Fouser LA, Artis D. 2011. Border patrol: regulation of immunity, inflammation and tissue homeostasis at barrier surfaces by IL-22. Nat Immunol 12(5):383–390, PMID: 21502992, https://doi.org/10.1038/ni.2025.
40. Zheng Y, Valdez PA, Danilenko DM, Hu Y, Sa SM, Gong Q, et al. 2008. Interleukin-22 mediates early host defense against attaching and effacing bacterial pathogens. Nat Med 14(3):282–289, PMID: 18264109, https://doi.org/10.1038/nm1720.
41. Figliuolo VR, Dos Santos LM, Abalo A, Nanini H, Santos A, Brittes NM, et al. 2017. Sulfate-reducing bacteria stimulate gut immune responses and contribute to inflammation in experimental colitis. Life Sci 189:29–38, PMID: 28912045, https://doi.org/10.1016/j.lfs.2017.09.014.
42. Aparicio-Domingo P, Romera-Hernandez M, Karrich JJ, Cornelissen F, Papazian N, Lindenbergh-Kortleve DJ, et al. 2015. Type 3 innate lymphoid cells maintain intestinal epithelial stem cells after tissue damage. J Exp Med 212(11):1783–1791, PMID: 26392223, https://doi.org/10.1084/jem.20150318.
43. Okamura T, Hamaguchi M, Mori J, Yamaguchi M, Mizushima K, Abe A, et al. 2022. Partially hydrolyzed guar gum suppresses the development of sarcopenic obesity. Nutrients 14(6):1157, PMID: 35334814, https://doi.org/10.3390/NU14061157.
44. Kawano R, Okamura T, Hashimoto Y, Majima S, Senmaru T, Ushigome E, et al. 2021. Erythritol ameliorates small intestinal inflammation induced by high-fat diets and improves glucose tolerance. Int J Mol Sci 22(11):5558, https://doi.org/10.3390/ijms22115558.
45. Kiela PR, Ghishan FK. 2016. Physiology of intestinal absorption and secretion. Best Pract Res Clin Gastroenterol 30(2):145–159, PMID: 27086882, https://doi.org/10.1016/j.bpg.2016.02.007.
46. Kolodziejczyk AA, Zheng D, Shibolet O, Elinav E. 2019. The role of the microbiome in NAFLD and NASH. EMBO Mol Med 11(2):e9302, PMID: 30591521, https://doi.org/10.15252/EMMM.201809302.
47. Dai X, Wang B. 2015. Role of gut barrier function in the pathogenesis of nonalcoholic fatty liver disease. Gastroenterol Res Pract 2015:287348, PMID: 25945084, https://doi.org/10.1155/2015/287348.
48. Hamaguchi M, Kojima T, Takeda N, Nakagawa T, Taniguchi H, Fujii K, et al. 2005. The metabolic syndrome as a predictor of nonalcoholic fatty liver disease. Ann Intern Med 143(10):722–728, PMID: 16287793, https://doi.org/10.7326/0003-4819-143-10-200511150-00009.
49. Yang YF, Chen C-Y, Lu T-H, Liao C-M. 2019. Toxicity-based toxicokinetic/toxicodynamic assessment for bioaccumulation of polystyrene microplastics in mice. J Hazard Mater 366:703–713, PMID: 30583240, https://doi.org/10.1016/j.jhazmat.2018.12.048.
50. Jin Y, Xia J, Pan Z, Yang J, Wang W, Fu Z. 2018. Polystyrene microplastics induce microbiota dysbiosis and inflammation in the gut of adult zebrafish. Environ Pollut 235:322–329, PMID: 29304465, https://doi.org/10.1016/j.envpol.2017.12.088.
51. Kawai S, Takagi Y, Kaneko S, Kurosawa T. 2011. Effect of three types of mixed anesthetic agents alternate to ketamine in mice. Exp Anim 60(5):481–487, PMID: 22041285, https://doi.org/10.1538/expanim.60.481.
52. McGowan MW, Artiss JD, Strandbergh DZ, Zak B. 1983. A peroxidase-coupled method for the colorimetric determination of serum triglycerides. Clin Chem 29(3):538–542, 6825269, https://doi.org/10.1093/clinchem/29.3.538.
53. Christmass MA, Mitoulas LR, Hartmann PE, Arthur PG. 1998. A semiautomated enzymatic method for determination of nonesterified fatty acid concentration in milk and plasma. Lipids 33(10):1043–1049, PMID: 9832086, https://doi.org/10.1007/s11745-998-0304-9.
54. Allain CC, Poon LS, Chan CS, Richmond W, Fu PC. 1974. Enzymatic determination of total serum cholesterol. Clin Chem 20(4):470–475, PMID: 4818200, https://doi.org/10.1093/clinchem/20.4.470.
55. Okamura T, Nakajima H, Hashimoto Y, Majima S, Senmaru T, Ushigome E, et al. 2021. Low circulating dihomo-gamma-linolenic acid is associated with diabetic retinopathy: a cross sectional study of KAMOGAWA-DM cohort study. Endocr J 68(4):421–428, PMID: 33361692, https://doi.org/10.1507/endocrj.EJ20-0564.
56. Motta J-P, Flannigan KL, Agbor TA, Beatty JK, Blackler RW, Workentine ML, et al. 2015. Hydrogen sulfide protects from colitis and restores intestinal microbiota biofilm and mucus production. Inflamm Bowel Dis 21(5):1006–1017, PMID: 25738373, https://doi.org/10.1097/MIB.0000000000000345.
57. Keinänen O, Dayts EJ, Rodriguez C, Sarrett SM, Brennan JM, Sarparanta M, et al. 2021. Harnessing PET to track micro- and nanoplastics in vivo. Sci Rep 11(1):11463, PMID: 34075133, https://doi.org/10.1038/S41598-021-90929-6.

58. Tenuta T, Monopoli MP, Kim JA, Salvati A, Dawson KA, Sandin P, et al. 2011. Elution of labile fluorescent dye from nanoparticles during biological use. PLoS One 6(10):e25556, PMID: 21998668, https://doi.org/10.1371/journal.pone.0025556.
59. Widner DB, Liu C, Zhao Q, Sharp S, Eber MR, Park SH, et al. 2021. Activated mast cells in skeletal muscle can be a potential mediator for cancer-associated cachexia. J Cachexia Sarcopenia Muscle. 12(4):1079–1097, PMID: 34008339, https://doi.org/10.1002/JCSM.12714.
60. Molofsky AB, Nussbaum JC, Liang H-E, Van Dyken SJ, Cheng LE, Mohapatra A, et al. 2013. Innate lymphoid type 2 cells sustain visceral adipose tissue eosinophils and alternatively activated macrophages. J Exp Med 210(3):535–549, PMID: 23420878, https://doi.org/10.1084/jem.20121964.
61. Wang S, Li J, Wu S, Cheng L, Shen Y, Ma W, et al. 2018. Type 3 innate lymphoid cell: a new player in liver fibrosis progression. Clin Sci (Lond) 132(24):2565–2582, PMID: 30459204, https://doi.org/10.1042/CS20180482.
62. Ono Y, Nagai M, Yoshino O, Koga K, Nawaz A, Hatta H, et al. 2018. CD11c+ M1-like macrophages (MΦs) but not CD206+ M2-like MΦ are involved in folliculogenesis in mice ovary. Sci Rep 8(1):8171, PMID: 29802255, https://doi.org/10.1038/s41598-018-25837-3.
63. Kleiner DE, Brunt EM, Van Natta M, Behling C, Contos MJ, Cummings OW, et al. 2005. Design and validation of a histological scoring system for nonalcoholic fatty liver disease. Hepatology 41(6):1313–1321, PMID: 15915461, https://doi.org/10.1002/hep.20701.
64. Caporaso JG, Kuczynski J, Stombaugh J, Bittinger K, Bushman FD, Costello EK, et al. 2010. QIIME allows analysis of high-throughput community sequencing data. Nat Methods 7(5):335–336, PMID: 20383131, https://doi.org/10.1038/nmeth.f.303.
65. Edgar RC. 2010. Search and clustering orders of magnitude faster than BLAST. Bioinformatics 26(19):2460–2461, PMID: 20709691, https://doi.org/10.1093/bioinformatics/btq461.
66. Chao A, Chazdon RL, Colwell RK, Shen TJ. 2006. Abundance-based similarity indices and their estimation when there are unseen species in samples. Biometrics 62(2):361–371, PMID: 16918900, https://doi.org/10.1111/j.1541-0420.2005.00489.x.
67. Shannon CE, Weaver W. 1949. *The Mathematical Theory of Communication*. Champagne, IL: University of Illinois Press, 1–117.
68. Simpson EH. 1949. Measurement of diversity. Nature 163(4148):688–688, https://doi.org/10.1038/163688a0.
69. Segata N, Izard J, Waldron L, Gevers D, Miropolsky L, Garrett WS, et al. 2011. Metagenomic biomarker discovery and explanation. Genome Biol 12(6):R60, PMID: 21702898, https://doi.org/10.1186/gb-2011-12-6-r60.
70. Nakanishi Y, Duran A, L'Hermitte A, Shelton PM, Nakanishi N, Reina-Campos M, et al. 2018. Simultaneous loss of both atypical protein kinase C genes in the intestinal epithelium drives serrated intestinal cancer by impairing immunosurveillance. Immunity 49(6):1132–1147.e7, PMID: 30552022, https://doi.org/10.1016/j.immuni.2018.09.013.
71. Chiang HY, Lu HH, Sudhakar JN, et al. 2022. IL-22 initiates an IL-18-dependent epithelial response circuit to enforce intestinal host defence. Nat Commun 13(1):874, PMID: 35169117, https://doi.org/10.1038/S41467-022-28478-3.
72. Bernink JH, Peters CP, Munneke M, Te Velde AA, Meijer SL, Weijer K, et al. 2013. Human type 1 innate lymphoid cells accumulate in inflamed mucosal tissues. Nat Immunol 14(3):221–229, PMID: 23334791, https://doi.org/10.1038/ni.2534.
73. Forkel M, van Tol S, Höög C, Michaëlsson J, Almer S, Mjösberg J. 2019. Distinct Alterations in the composition of mucosal innate lymphoid cells in newly diagnosed and established Crohn's disease and ulcerative colitis. J Crohns Colitis 13(1):67–78, PMID: 30496425, https://doi.org/10.1093/ecco-jcc/jjy119.
74. Rankin LC, Girard-Madoux MJH, Seillet C, Mielke LA, Kerdiles Y, Fenis A, et al. 2016. Complementarity and redundancy of IL-22-producing innate lymphoid cells. Nat Immunol 17(2):179–186, PMID: 26595889, https://doi.org/10.1038/ni.3332.
75. Ijssennagger N, van der Meer R, van Mil SWC. 2016. Sulfide as a mucus Barrier-Breaker in inflammatory bowel disease? Trends Mol Med 22(3):190–199, PMID: 26852376, https://doi.org/10.1016/j.molmed.2016.01.002.
76. Mills CD, Kincaid K, Alt JM, Heilman MJ, Hill AM. 2000. M-1/M-2 macrophages and the Th1/Th2 paradigm. J Immunol 164(12):6166–6173, PMID: 10843666, https://doi.org/10.4049/jimmunol.164.12.6166.
77. Yang W, Yu T, Huang X, Bilotta AJ, Xu L, Lu Y, et al. 2020. Intestinal microbiota-derived short-chain fatty acids regulation of immune cell IL-22 production and gut immunity. Nat Commun 11(1):4457, https://doi.org/PMID: 32901017, https://doi.org/10.1038/S41467-020-18262-6.
78. Tolhurst G, Heffron H, Lam YS, Parker HE, Habib AM, Diakogiannaki E, et al. 2012. Short-chain fatty acids stimulate glucagon-like peptide-1 secretion via the G-protein-coupled receptor FFAR2. Diabetes 61(2):364–371, PMID: 22190648, https://doi.org/10.2337/db11-1019.
79. Brown AJ, Goldsworthy SM, Barnes AA, Eilert MM, Tcheang L, Daniels D, et al. 2003. The Orphan G protein-coupled receptors GPR41 and GPR43 are activated by propionate and other short chain carboxylic acids. J Biol Chem 278(13):11312–11319, PMID: 12496283, https://doi.org/10.1074/jbc.M211609200.
80. Schütte A, Ermund A, Becker-Pauly C, Johansson MEV, Rodriguez-Pineiro AM, Bäckhed F, et al. 2014. Microbial-induced meprin β cleavage in MUC2 mucin and a functional CFTR channel are required to release anchored small intestinal mucus. Proc Natl Acad Sci U S A 111(34):12396–12401, PMID: 25114233, https://doi.org/10.1073/pnas.1407597111.
81. Borisova MA, Achasova KM, Morozova KN, Andreyeva EN, Litvinova EA, Ogienko AA, et al. 2020. Mucin-2 knockout is a model of intercellular junction defects, mitochondrial damage and ATP depletion in the intestinal epithelium. Sci Rep 10(1):21135, PMID: 33273633, https://doi.org/10.1038/S41598-020-78141-4.
82. Yan Z, Liu Y, Zhang T, Zhang F, Ren H, Zhang Y. 2021. Analysis of microplastics in human feces reveals a correlation between fecal microplastics and inflammatory bowel disease status. Environ Sci Technol 56(1):414–421, PMID: 34935363, https://doi.org/10.1021/ACS.EST.1C03924.
83. Al-Sadi R, Boivin M, Ma T. 2009. Mechanism of cytokine modulation of epithelial tight junction barrier. Front Biosci (Landmark Ed) 14(7):2765–2778, PMID: 19273235, https://doi.org/10.2741/3413.
84. Ludwiczek O, Vannier E, Borggraefe I, Kaser A, Siegmund B, Dinarello CA, et al. 2004. Imbalance between interleukin-1 agonists and antagonists: relationship to severity of inflammatory bowel disease. Clin Exp Immunol 138(2):323–329, PMID: 15498044, https://doi.org/10.1111/j.1365-2249.2004.02599.x.
85. Al-Sadi RM, Ma TY. 2007. IL-1beta causes an increase in intestinal epithelial tight junction permeability. J Immunol 178(7):4641–4649, PMID: 17372023, https://doi.org/10.4049/jimmunol.178.7.4641.
86. Ma TY, Iwamoto GK, Hoa NT, Akotia V, Pedram A, Boivin MA, et al. 2004. TNF-alpha-induced increase in intestinal epithelial tight junction permeability requires NF-kappa B activation. Am J Physiol Gastrointest Liver Physiol 286(3):G367–G376, PMID: 14766535, https://doi.org/10.1152/AJPGI.00173.2003.
87. Artis D, Spits H. 2015. The biology of innate lymphoid cells. Nature 517(7534):293–301, PMID: 25592534, https://doi.org/10.1038/nature14189.
88. Turner JE, Stockinger B, Helmby H. 2013. IL-22 mediates goblet cell hyperplasia and worm expulsion in intestinal helminth infection. PLoS Pathog 9(10):e1003698, PMID: 24130494, https://doi.org/10.1371/JOURNAL.PPAT.1003698.
89. Chun E, Lavoie S, Fonseca-Pereira D, Bae S, Michaud M, Hoveyda HR, et al. 2019. Metabolite-sensing receptor Ffar2 regulates colonic group 3 innate lymphoid cells and gut immunity. Immunity 51(5):871–884.e6, PMID: 31628054, https://doi.org/10.1016/j.immuni.2019.09.014.
90. Sepahi A, Liu QY, Friesen L, Kim CH. 2021. Dietary fiber metabolites regulate innate lymphoid cell responses. Mucosal Immunol 14(2):317–330, PMID: 32541842, https://doi.org/10.1038/s41385-020-0312-8.
91. Fachi JL, Sécca C, Rodrigues PB, Pinheiro de Mato FC, Di Luccia B, de Souza Felipe J, et al. 2020. Acetate coordinates neutrophil and ILC3 responses against C. difficile through FFAR2. J Exp Med 217(3):jem.20190489, PMID: 31876919, https://doi.org/10.1084/jem.20190489.
92. Vieira ELM, Leonel AJ, Sad AP, Beltrão NRM, Costa TF, Ferreira TMR, et al. 2012. Oral administration of sodium butyrate attenuates inflammation and mucosal lesion in experimental acute ulcerative colitis. J Nutr Biochem 23(5):430–436, PMID: 21658926, https://doi.org/10.1016/j.jnutbio.2011.01.007.
93. Gao Z, Yin J, Zhang J, Ward RE, Martin RJ, Lefevre M, et al. 2009. Butyrate improves insulin sensitivity and increases energy expenditure in mice. Diabetes 58(7):1509–1517, PMID: 19366864, https://doi.org/10.2337/db08-1637.
94. Rodríguez-Cabezas ME, Gálvez J, Lorente MD, Concha A, Camuesco D, Azzouz S, et al. 2002. Dietary fiber down-regulates colonic tumor necrosis factor alpha and nitric oxide production in trinitrobenzenesulfonic acid-induced colitic rats. J Nutr 132(11):3263–3271, PMID: 12421838, https://doi.org/10.1093/jn/132.11.3263.
95. Tarrerias AL, Millecamps M, Alloui A, Beaughard C, Kemeny JL, Bourdu S, et al. 2002. Short-chain fatty acid enemas fail to decrease colonic hypersensitivity and inflammation in TNBS-induced colonic inflammation in rats. Pain 100(1–2):91–97, PMID: 12435462, https://doi.org/10.1016/S0304-3959(02)00234-8.
96. Yamashita H, Fujisawa K, Ito E, Idei S, Kawaguchi N, Kimoto M, et al. 2007. Improvement of obesity and glucose tolerance by acetate in type 2 diabetic Otsuka Long-Evans Tokushima fatty (OLETF) rats. Biosci Biotechnol Biochem 71(5):1236–1243, PMID: 17485860, https://doi.org/10.1271/bbb.60668.
97. Scheppach W, Sommer H, Kirchner T, Paganelli GM, Bartram P, Christl S, et al. 1992. Effect of butyrate enemas on the colonic mucosa in distal ulcerative colitis. Gastroenterology 103(1):51–56, PMID: 1612357, https://doi.org/10.1016/0016-5085(92)91094-K.
98. Hamer HM, Jonkers DMAE, Vanhoutvin SALW, Troost FJ, Rijkers G, de Bruïne A, et al. 2010. Effect of butyrate enemas on inflammation and antioxidant status in the colonic mucosa of patients with ulcerative colitis in remission. Clin Nutr 29(6):738–744, PMID: 20471725, https://doi.org/10.1016/j.clnu.2010.04.002.
99. Vernia P, Annese V, Bresci G, d'Albasio G, D'Incà R, Giaccari S, et al. 2003. Topical butyrate improves efficacy of 5-ASA in refractory distal ulcerative colitis: results of a multicentre trial. Eur J Clin Invest 33(3):244–248, PMID: 12641543, https://doi.org/10.1046/j.1365-2362.2003.01130.x.

100. Lin H. V, Frassetto A, Kowalik EJ Jr, Nawrocki AR, Lu MM, Kosinski JR, et al. 2012. Butyrate and propionate protect against diet-induced obesity and regulate gut hormones via free fatty acid receptor 3-independent mechanisms. PLoS One 7(4):e35240, PMID: 22506074, https://doi.org/10.1371/journal.pone.0035240.
101. Shin NR, Whon TW, Bae JW. 2015. Proteobacteria: microbial signature of dysbiosis in gut microbiota. Trends Biotechnol 33(9):496–503, PMID: 26210164, https://doi.org/10.1016/j.tibtech.2015.06.011.
102. Méndez-Salazar EO, Ortiz-López MG, Granados-Silvestre MDLÁ, Palacios-González B, Menjivar M. 2018. Altered Gut microbiota and compositional changes in *Firmicutes* and P*roteobacteria* in Mexican undernourished and obese children. Front Microbiol 9:2494, PMID: 30386323, https://doi.org/10.3389/FMICB.2018.02494.
103. Mangin I, Bonnet R, Seksik P, Rigottier-Gois L, Sutren M, Bouhnik Y, et al. 2004. Molecular inventory of faecal microflora in patients with Crohn's disease. FEMS Microbiol Ecol 50(1):25–36, PMID: 19712374, https://doi.org/10.1016/j.femsec.2004.05.005.
104. Gophna U, Sommerfeld K, Gophna S, Doolittle WF, Veldhuyzen Van Zanten SJO. 2006. Differences between tissue-associated intestinal microfloras of patients with Crohn's disease and ulcerative colitis. J Clin Microbiol 44(11):4136–4141, PMID: 16988016, https://doi.org/10.1128/JCM.01004-06.
105. Lavelle A, Lennon G, O'Sullivan O, Docherty N, Balfe A, Maguire A, et al. 2015. Spatial variation of the colonic microbiota in patients with ulcerative colitis and control volunteers. Gut 64(10):1553–1561, PMID: 25596182, https://doi.org/10.1136/gutjnl-2014-307873.
106. Volynets V, Louis S, Pretz D, Lang L, Ostaff MJ, Wehkamp J, et al. 2017. Intestinal barrier function and the gut microbiome are differentially affected in mice fed a Western-style diet or drinking water supplemented with fructose. J Nutr 147(5):770–780, PMID: 28356436, https://doi.org/10.3945/jn.116.242859.
107. Cho KY. 2021. Lifestyle modifications result in alterations in the gut microbiota in obese children. BMC Microbiol 21(1):10, PMID: 33407104, https://doi.org/10.1186/S12866-020-02002-3.
108. Schnorr SL, Candela M, Rampelli S, Consolandi C, Basaglia G, Turroni S, et al. 2014. Gut microbiome of the Hadza hunter-gatherers. Nat Commun 5:3654, PMID: 24736369, https://doi.org/10.1038/NCOMMS4654.
109. Downes J, Dewhirst FE, Tanner ACR, Wade WG. 2013. Description of *Alloprevotella rava* gen. nov., sp. nov., isolated from the human oral cavity, and reclassification of *Prevotella tannerae* Moore et al. 1994 as *Alloprevotella tannerae* gen. nov., comb. nov. Int J Syst Evol Microbiol 63(Pt 4):1214–1218, PMID: 22753527, https://doi.org/10.1099/ijs.0.041376-0.
110. Kong C, Gao R, Yan X, Huang L, Qin H. 2019. Probiotics improve gut microbiota dysbiosis in obese mice fed a high-fat or high-sucrose diet. Nutrition 60:175–184, PMID: 30611080, https://doi.org/10.1016/j.nut.2018.10.002.
111. Kreutzer C, Peters S, Schulte DM, Fangmann D, Türk K, Wolff S, et al. 2017. Hypothalamic Inflammation in human obesity is mediated by environmental and genetic factors. Diabetes 66(9):2407–2415, PMID: 28576837, https://doi.org/10.2337/db17-0067.
112. Zhang C, Zhang M, Pang X, Zhao Y, Wang L, Zhao L. 2012. Structural resilience of the gut microbiota in adult mice under high-fat dietary perturbations. ISME J 6(10):1848–1857, PMID: 22495068, https://doi.org/10.1038/ismej.2012.27.
113. Xie G, Wang X, Huang F, Zhao A, Chen W, Yan J, et al. 2016. Dysregulated hepatic bile acids collaboratively promote liver carcinogenesis. Int J Cancer 139(8):1764–1775, PMID: 27273788, https://doi.org/10.1002/ijc.30219.
114. Danneskiold-Samsøe NB, Andersen D, Radulescu ID, Normann-Hansen A, Brejnrod A, Kragh M, et al. 2017. A safflower oil based high-fat/high-sucrose diet modulates the gut microbiota and liver phospholipid profiles associated with early glucose intolerance in the absence of tissue inflammation. Mol Nutr Food Res 61(5), PMID: 28012235, https://doi.org/10.1002/MNFR.201600528.
115. Ibrahim KS, Bourwis N, Dolan S, Lang S, Spencer J, Craft JA. 2021. Characterisation of gut microbiota of obesity and type 2 diabetes in a rodent model. Biosci Microbiota Food Health 40(1):65–74, PMID: 33520571, https://doi.org/10.12938/bmfh.2019-031.
116. Krych Ł, Nielsen DS, Hansen AK, Hansen CHF. 2015. Gut microbial markers are associated with diabetes onset, regulatory imbalance, and IFN-γ level in NOD mice. Gut Microbes 6(2):101–109, PMID: 25648687, https://doi.org/10.1080/19490976.2015.1011876.
117. Qin J, Li Y, Cai Z, Li S, Zhu J, Zhang F, et al. 2012. A metagenome-wide association study of gut microbiota in type 2 diabetes. Nature 490(7418):55–60, PMID: 23023125, https://doi.org/10.1038/nature11450.
118. Petersen C, Bell R, Klag KA, Lee S-H, Soto R, Ghazaryan A, et al. 2019. T cell-mediated regulation of the microbiota protects against obesity. Science 365(6451):eaat9351, PMID: 31346040, https://doi.org/10.1126/science.aat9351.
119. Le Chatelier E, Nielsen T, Qin J, Prifti E, Hildebrand F, Falony G, et al. 2013. Richness of human gut microbiome correlates with metabolic markers. Nature 500(7464):541–546, PMID: 23985870, https://doi.org/10.1038/nature12506.
120. Pitt JA, Kozal JS, Jayasundara N, Massarsky A, Trevisan R, Geitner N, et al. 2018. Uptake, tissue distribution, and toxicity of polystyrene nanoparticles in developing zebrafish (*Danio rerio*). Aquat Toxicol 194:185–194, PMID: 29197232, https://doi.org/10.1016/j.aquatox.2017.11.017.
121. Pitt JA, Trevisan R, Massarsky A, Kozal JS, Levin ED, di Giulio RT. 2018. Maternal transfer of nanoplastics to offspring in zebrafish (*Danio rerio*): a case study with nanopolystyrene. Sci Total Environ 643:324–334, PMID: 29940444, https://doi.org/10.1016/j.scitotenv.2018.06.186.
122. Brun NR, van Hage P, Hunting ER, Haramis A-PG, Vink SC, Vijver MG, et al. 2019. Polystyrene nanoplastics disrupt glucose metabolism and cortisol levels with a possible link to behavioural changes in larval zebrafish. Commun Biol 2(1): PMID: 31646185, https://doi.org/10.1038/s42003-019-0629-6.